1962

Phase stabilization of traveling-wave tube shifters

Norman Saul Nise
Lehigh University

PHASE STABILIZATION
OF
TRAVELING-WAVE TUBE PHASE SHIFTERS

by
Norman Saul Nise

A THESIS

Presented to the Graduate Faculty

of Lehigh University

in Candidacy for the Degree of

Master of Science in Electrical Engineering

Lehigh University

1962

This thesis is accepted and approved in partial fulfillment of the requirements for the degree of Master of Science in Electrical Engineering.

March 16, 1962
(date)

John J. Karakash
Professor in charge

John J. Karakash
Head of the Department of
Electrical Engineering

ACKNOWLEDGEMENTS

The author wishes to thank the Hughes Aircraft Company, Ground Systems Group, for its cooperation in making available its facilities. In particular, thanks is extended to Mr. Gus Wershoven and Mr. Richard Boucher of the Radar Studies Department for their comments and suggestions concerning this report.

Acknowledgement is also given to Lehigh University for its award of the C. Kemble Baldwin Fellowship, without which, the author's graduate studies might never have been carried out.

Finally, the author wishes to thank Professor John J. Karakash, Head of the Department of Electrical Engineering at Lehigh University, for his guidance throughout the entire program.

TABLE OF CONTENTS

LIST OF FIGURES

ABSTRACT

This thesis deals with the design and experimental results of a method for phase stabilizing a traveling-wave tube phase shifter used in pulsed-type radars.

Design criteria are presented in a general form so that the information can be applied to other design problems. Experimental results are shown for special cases.

The Bibliography and earlier chapters serve as an index for information pertaining to the phase stabilization of microwave tubes in general.

CHAPTER 1

INTRODUCTION

World War II radar systems are becoming outdated by modern radars employing fixed-array antennas. These new systems are capable of beam steering by varying the frequency and/or phase relation among members of an array. Phase programming is often accomplished by ferrite phase shifters which are highly temperature sensitive and require elaborate cooling systems. Further, amplification of the signal must take place elsewhere in the radar set.

Traveling-wave tubes are now being considered as an alternative for ferrite phase shifters since amplification and phase control can be accomplished with the same piece of hardware.

It is the object of this thesis to investigate ways of phase stabilizing traveling-wave tubes used as phase shifters. Chapter 2 deals with the basic theory of such use. Chapter 3 is an exposition of the state of the art of phase stabilizing microwave tubes. Chapters 4 and 5 are devoted to design and experimental results of a specific method of stabilization. The latter section of Chapter 5 concerns itself with conclusions and projections for further work.

CHAPTER 2

THE TRAVELING-WAVE TUBE (TWT)

In order to develop the basis for phase stabilization of traveling-wave tubes, it is necessary to begin with a discussion of operation of the tube. This chapter concerns itself, initially, with basic TWT theory and concludes with aspects of the theory of the traveling-wave tube when employed as a phase shifting device.

2.1 Introduction

The nature of the problems encountered in amplification of signals at microwave frequencies becomes apparent in the study of transit time devices utilizing velocity modulation as is demonstrated by the klystron. However, the narrow bandwidth and physical tuning properties of this tube initiated the search for an improved type of amplifier. With the development of the traveling-wave tube the difficulties presented by the klystron were overcome.

2.2 The Traveling-Wave Tube

The operation of the traveling-wave tube is characterized by a transfer of energy from a beam of electrons to a "slow wave". Consider an electromagnetic wave progressing along a helical winding as in Figure 2-1. Essentially the wave is traveling at the speed of light, but its velocity along the axis is less than that of the velocity of light and is determined by the circumference and pitch of the helical windings.

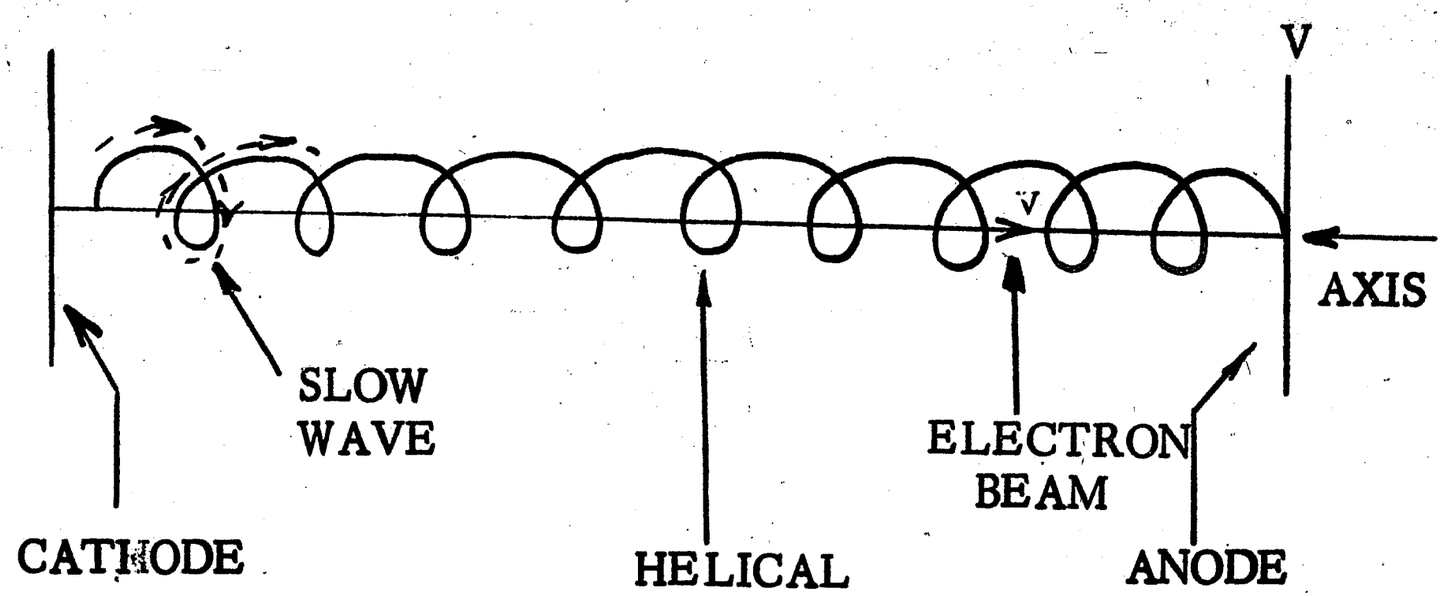

Fig. 2-1. Electromagnetic wave progressing along a helical winding.

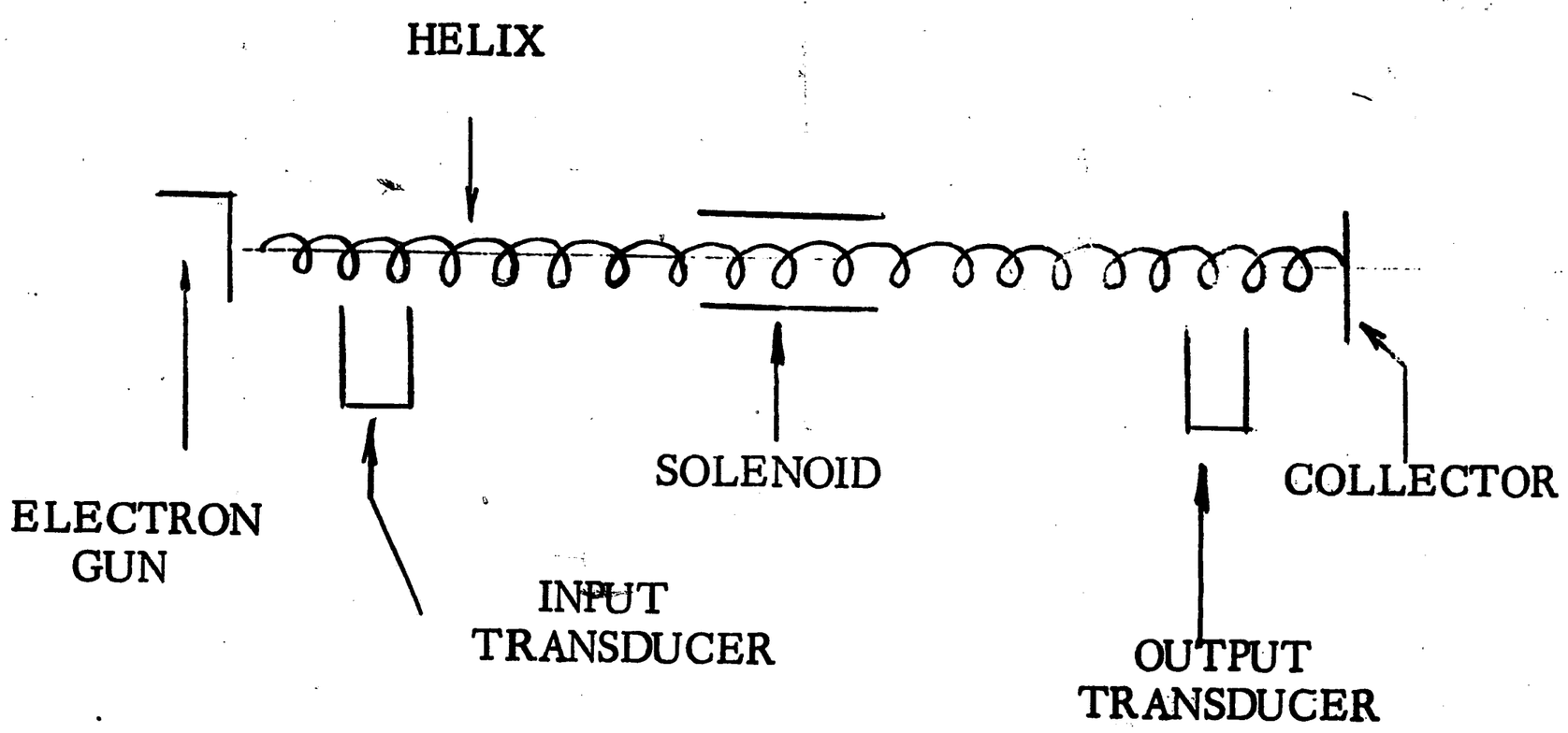

Fig. 2-2. Schematic diagram of TWT components. *1

1 RCA Electron Tube Division, "RCA Magnetrons and Traveling-Wave Tubes", Harrison N.J.; 1960.

Now, assume that a beam of electrons is directed along the axis at a velocity, v, determined by a potential difference from cathode to anode, V. Since the "slow wave" is electromagnetic energy, the beam of electrons will be accelerated or decelerated depending upon the sign of the field set up by the "slow wave". If the cathode to anode voltage is adjusted to cause the electron velocity to equal the wave-axial velocity, the electrons, when in the retarding field of the wave, will give up kinetic energy to the "slow wave". Thus, the helical axis must be several wave-lengths long in order for successive retarding fields to transfer enough energy from the beam to the wave to accomplish useful amplification.

The modern traveling-wave tube shown schematically in Figure 2-2 consists of an electron gun and a collector which accomplish the same function as the cathode and anode, respectively, of Figure 2-1. The helical winding is called a helix and the solenoid is employed to keep the electron stream focused as a thin beam on the collector. In some traveling-wave tubes the helix and the collector might be tied together and thus the beam velocity is a function of the helix voltage. Consequently, the helix voltage will be used to refer to that potential affecting the beam velocity.

2.3 The Traveling-Wave Tube as a Phase Shifter

Among the variables affecting the phase relation between the input and output signals in a traveling-wave tube are helix voltage, anode voltage, and solenoid current.

The phase sensitivity of the TWT to changes in anode voltage is developed in Appendix 2-1. The high sensitivity of the helix for producing phase changes makes the utilization of this element most desirable in the attempt at phase stabilization and extremely important with regard to phase shifting theory. Thus, the derivation of the phase sensitivity of the helix is included here in the body of the report rather than in the Appendices.

Derivation of the phase sensitivity of the helix of a TWT [1,2]

The phase constant of a wave through a TWT is defined as

$$\beta = \beta_e(1 - Cy), \qquad (1)$$

where

$\beta_e = \frac{\omega}{v_e}$ = phase constant of the electron beam of velocity, v_e,

C = gain parameter defined by Pierce; a function of beam impedance, magnitude of the field, power flow in the circuit and electron phase constant,

and y = function of average electron velocity.

Whereas the previous equation describes the phase constant for a wave disturbed by the presence of electrons, Pierce shows that

$$\beta_1 = \beta_e(1 + Cb) \qquad (2)$$

approximates the phase constant for a wave undisturbed by the presence of electrons. Here, b is a measure of velocity difference between the beam and the "slow wave".

Now, the average velocity of the beam is related to the helix voltage (beam voltage) as

1. Pierce, J. R., "Traveling-Wave Tubes", D. Van Nostrand, New York, N.Y.; 1950.
2. Beam, W. R. and Blattner, D. J., "Phase Angle Distortion in Traveling-Wave Tubes", RCA Review; March, 1956.

$$v_e = \sqrt{\frac{2e}{m_e} V_o}\ , \qquad (3)$$

where V_o = Beam Voltage,

e = electron charge,

and m_e = electron mass.

Therefore $$\frac{d v_e}{d V_o} = \frac{1}{2} \frac{v_e}{V_o} \qquad (4)$$

$$\approx \frac{\Delta v_e}{\Delta V_o}\ . \qquad (5)$$

Since $$v_e = \frac{\omega}{\beta_e} \qquad (6)$$

and $$\frac{\Delta_{v_e}}{\Delta \beta_e} = - \frac{\omega}{\beta_e^2}\ , \qquad (7)$$

$$\frac{\Delta \beta_e}{\beta_e} = - \frac{1}{2} \frac{\Delta V_o}{V_o}\ . \qquad (8)$$

For any specific tube, β_1 is constant, and hence from equation (2)

$$\Delta \beta_1 = 0 = \Delta \beta_e (1 + Cb) + \beta_e (C \Delta b). \qquad (9)$$

Therefore

$$\frac{\Delta \beta_e}{\beta_e} = - \frac{C \Delta b}{1 + Cb} \qquad (10)$$

and from (8)

$$\frac{C \Delta b}{1 + Cb} = \frac{1}{2} \frac{\Delta V_o}{V_o}\ . \qquad (11)$$

Beam and Blattner give the following approximation to Pierce's plot of y

$$y = -(.42 + .07\ QC)b - (.5 + .5\ QC). \tag{12}$$

From this, we obtain

$$\Delta y = -.(42 + .07\ QC)\Delta b, \tag{13}$$

where Q is a space charge parameter.

Also, from (1),

$$\Delta \beta = \Delta \beta_e(1 - Cy) + \beta_e(-Cy). \tag{14}$$

Combining (8), (11), (13), and (14),

$$\Delta \beta = \frac{\Delta V_o}{2 V_o} \beta_e([1 + bC][.42 + .07\ QC] + Cy - 1). \tag{15}$$

The change in phase angle is thus

$$\Delta \phi = \Delta \beta \cdot L, \tag{16}$$

where L is the circuit length.

Upon substitution in (15), the result is

$$\Delta \phi = \frac{\Delta V_o}{V_o} \pi([1 + bC][.42 + .07\ QC] + Cy - 1)N, \tag{17}$$

where N is L in wavelengths.

Pierce[1] shows that reduction of gain is minimized when QC is much less than one. Thus for a typical traveling-wave tube ($y \approx b \approx 1$, $C \approx .01$), (17) reduces to

$$\Delta \phi \approx -105 \frac{\Delta V_o}{V_o} N \text{ degrees.}$$

This relationship is linear.

1. Pierce, J.R., "Traveling-Wave Tubes", D. Van Nostrand, New York, N.Y., p118; 1950.

2.4 Conclusions

The chapter establishes the fact that a traveling-wave tube can be used not only to amplify microwave signals, but to shift the phase of the output with respect to the input by controlling or programming the voltage on the helix. It was also shown that the phase sensitivity of the helix, within a first order approximation, is linear.

CHAPTER 3

METHODS FOR PHASE STABILIZATION OF TRAVELING-WAVE TUBES

This chapter deals with phase stabilization techniques, most of which were investigated by the Research Laboratory of Electronics at the Massachusetts Institute of Technology.[1, 2, 3] Although these closed-loop methods apply to systems where variable phase reference signals are applied for direct control, the discussion will serve as a preface for the detailed investigation of a phase-stabilized scheme without variable phase reference signals but with programmed helix voltages.

3.1 Introduction

In the contemplated use of traveling-wave tubes as phase shifters in fixed-array radars, it is of prime importance that the phase shift in each tube be kept at specified programmed values in order that electronic beam steering can be accomplished with the high accuracy needed in contemporary radar systems.

1. Research Laboratory of Electronics, MIT, "Phase Stabilization Techniques for Electronically Scanned Arrays", Quarterly Technical Note No. 1, AD 148 961, Cambridge, Massachusetts; September 15, 1958.
2. Research Laboratory of Electronics, MIT, "Phase Stabilization Techniques for Electronically Scanned Arrays", Quarterly Technical Note No. 2, AD 209 072, Cambridge, Massachusetts; December 15, 1958.
3. Research Laboratory of Electronics, MIT, "Phase Stabilization Techniques for Electronically Scanned Arrays", Quarterly Technical Note No. 3, AD 213 587, Cambridge, Massachusetts; March 15, 1959.

Changes in voltage or component values due to fluctuations in ambient or internal conditions must be kept to a minimum, or their effects neutralized. Neutralization is effected by phase stabilization techniques which insure minimum deviations from the programmed phase.

Basically, the techniques employed utilize a phase detector to measure the phase difference between input and output and a closed-loop for correction as shown in Figure 3-1.

3.2 Phase Detectors

The heart of any phase stabilization system is a device capable of translating a difference of phase into a voltage - the phase detector. This chapter concerns itself with the MIT methods while the next chapter covers other methods and leads to a choice of one to be incorporated in the design and test of a phase-stabilized TWT phase shifter.

3.3 Suppressed-Carrier Phase Detector

As shown in Figure 3-2, a suppressed-carrier-type phase detector consists, basically, of three devices. The adder sums two voltages represented in Figure 3-3, one of which is the signal output from the TWT at a frequency ω_c and the other is a reference input, suppressed-carrier modulated with a frequency ω_m.

It is observed that if the signal vector and the reference vector with its rotating sidebands are 90 degrees apart, there will not be any modulation in phase with the signal.

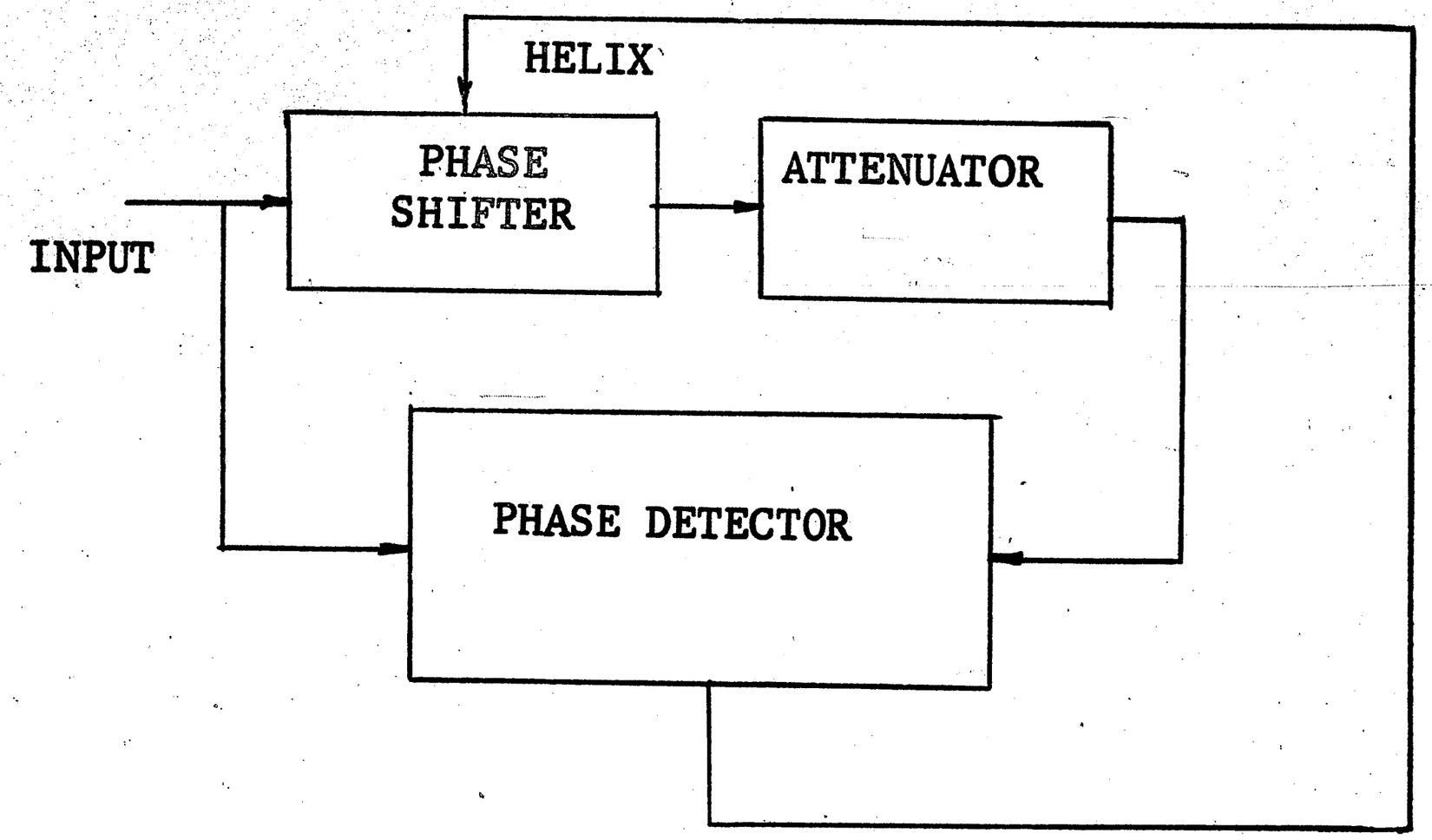

Fig. 3-1, A basic TWT phase correction scheme.

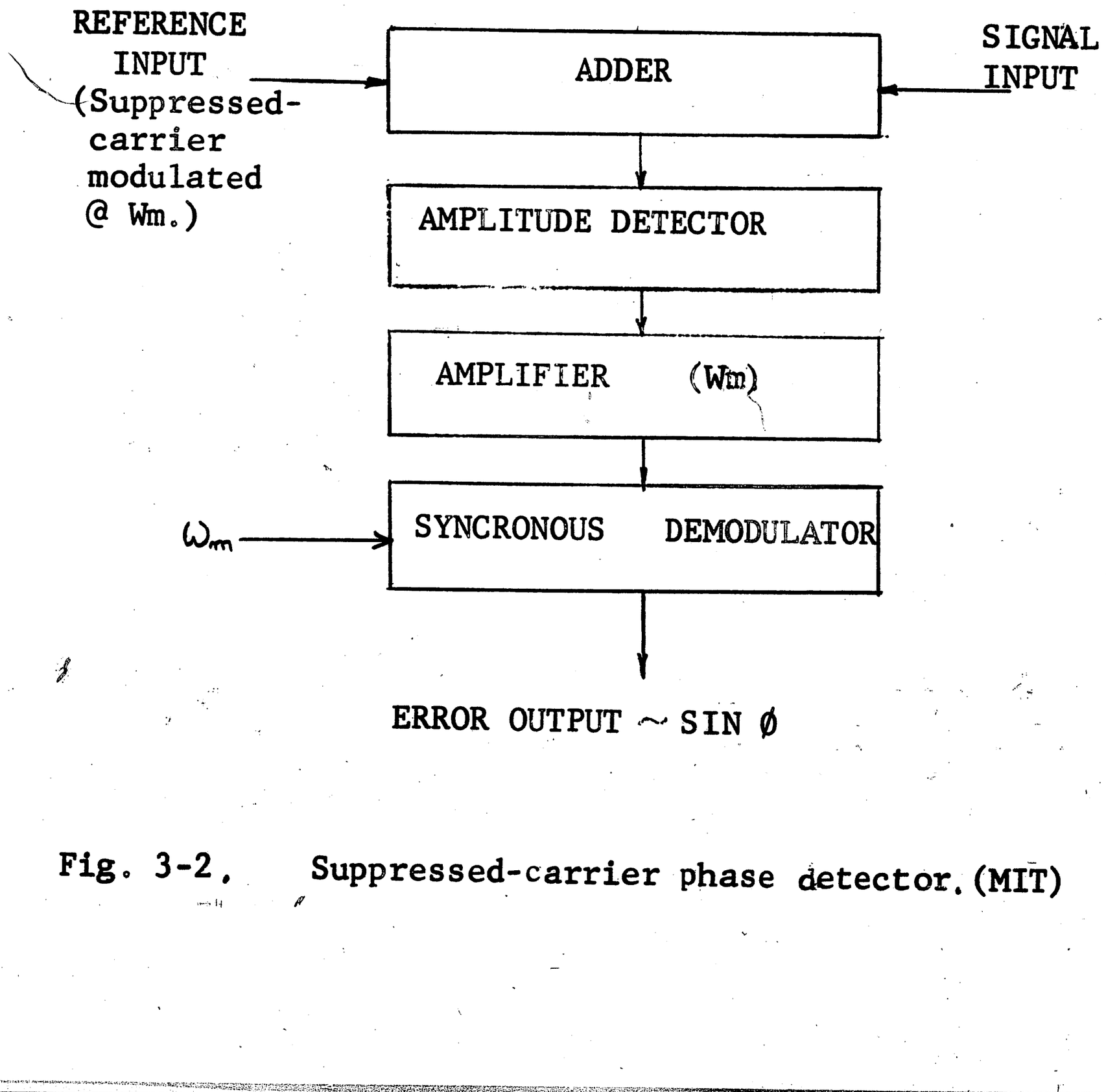

Fig. 3-2, Suppressed-carrier phase detector. (MIT)

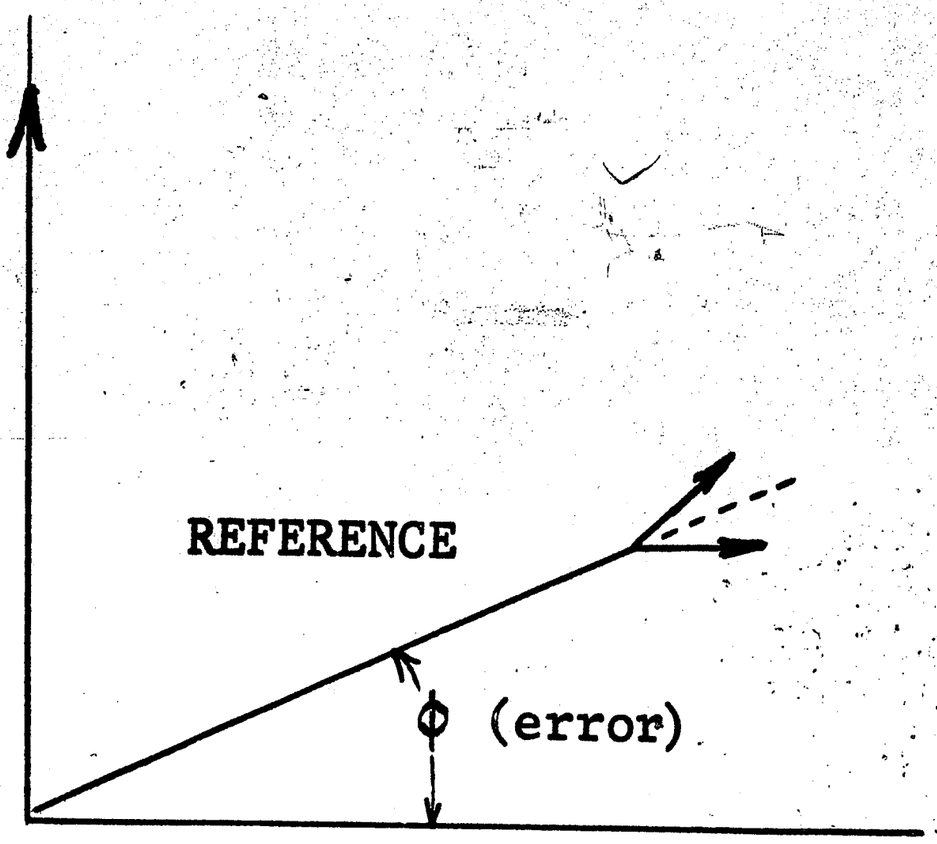

Fig. 3-3. Suppressed-carrier phase detector signal vector diagram. (MIT)

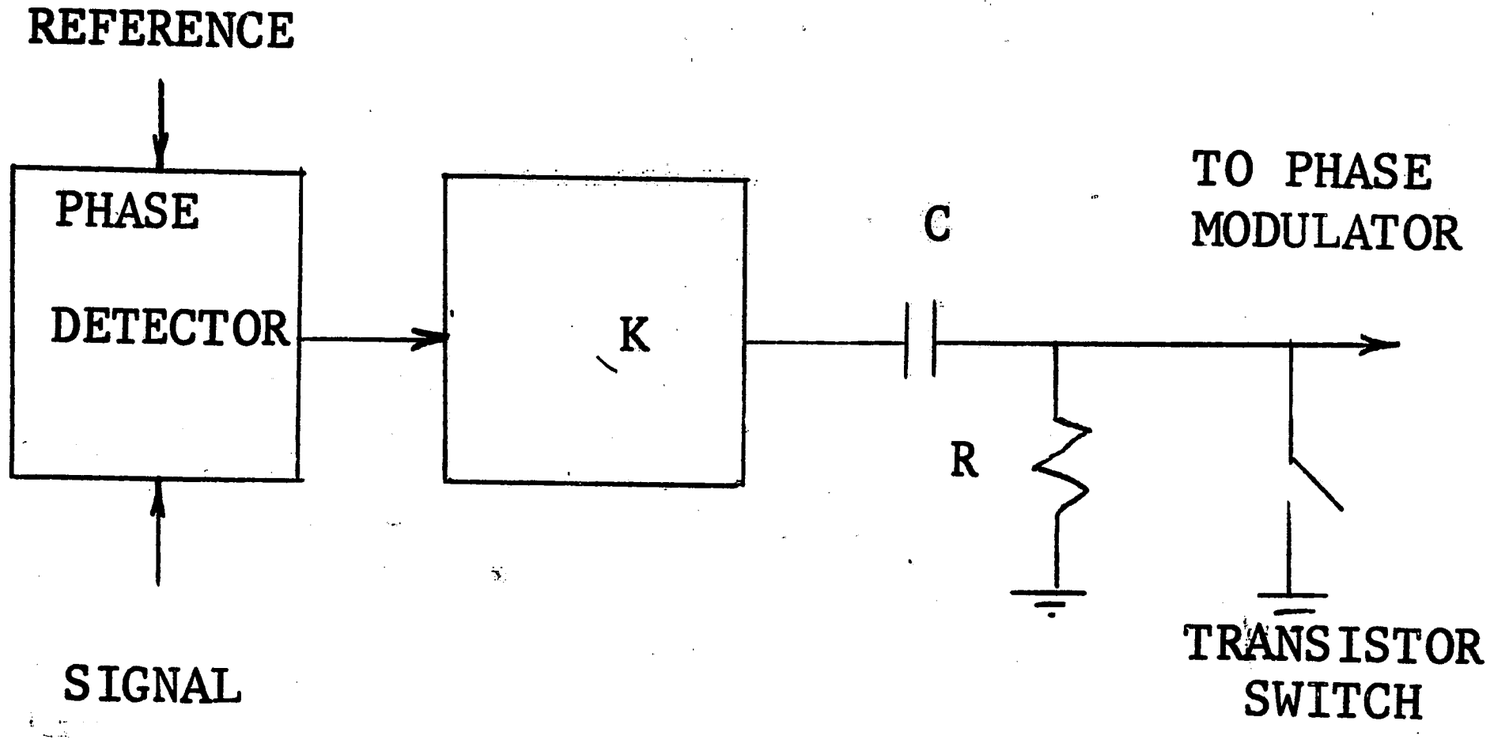

Fig. 3-4. Self-balancing phase detector scheme. (MIT)

Similarly, if the two vectors are in phase, then all of the modulation will appear in phase with the signal vector. Thus the phase difference ($\emptyset$) determines the amplitude of the modulation presented to the input signal. The amplitude detector then detects the modulation and the synchronous demodulator gives a d-c output related to the phase difference between signal and reference by detecting the amplitude of the modulating signal present. The relationship between phase difference and d-c voltage output from the phase detector approximates a sine curve.

3.4 Self-Balancing Phase Detector

A method of phase detection, especially applicable to pulsed radar systems, is a self-balancing phase detector, the block diagram of which is shown in Figures 3-4.

In radar systems where frequency changes from pulse to pulse, unbalances are likely to occur in a phase detector. In order to correct this condition, a transistor switch closes immediately before the radar pulse, and the unbalance charges up the capacitor C. Thus the capacitor voltage cancels the detector unbalance voltage. Figure 3-5 demonstrates the detailed operation of this phase detector. The input signal arrives at terminals 1 and 2 shifted 90 degrees so that

$$\bar{E}_1 = E_s e^{j\left(\frac{\pi}{2} + \theta\right)} + E_r e^{j0}$$

and

$$\bar{E}_2 = E_s e^{j\left(\frac{\pi}{2} + \theta\right)} + E_r e^{j\pi}$$

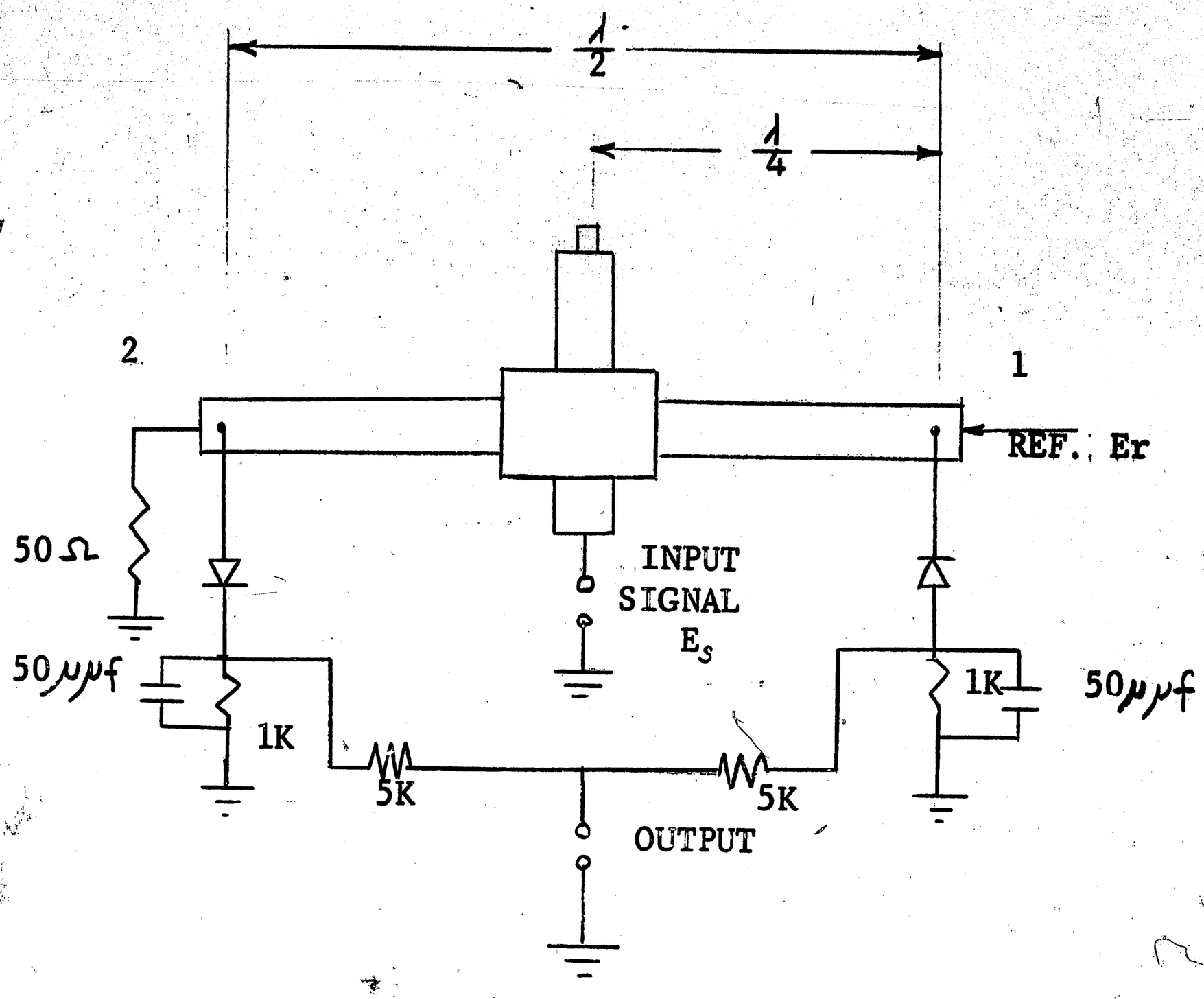

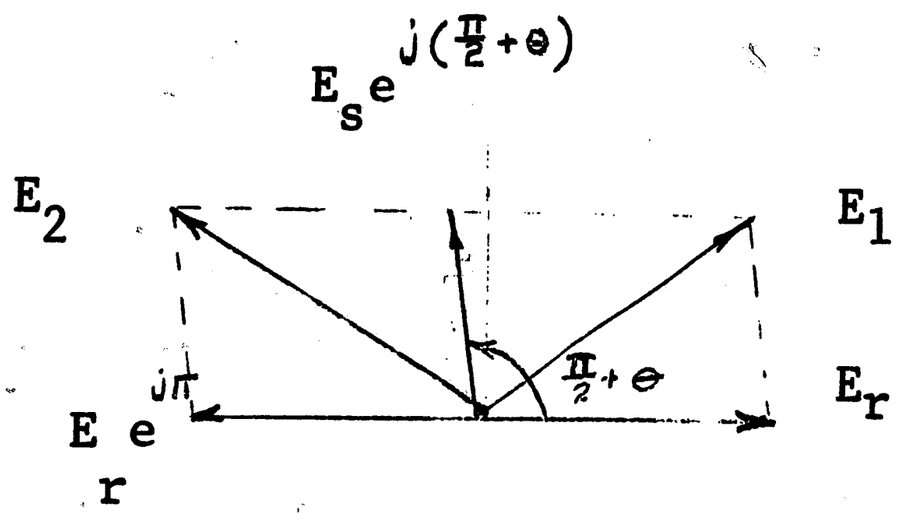

Fig. 3-5, Phase detector used in self-balancing scheme. (MIT)

The magnitude difference between $\bar{E}_1$ and $\bar{E}_2$ is related to the phase difference, θ, between signal and reference and thus phase detection is accomplished with the characteristic shown in Figure 3-6.

3.5 Employment of Phase Detectors in Closed-Loop Operation

Figure 3-7 shows the use of the suppressed-carrier modulated phase detector employed in closed-loop operation. The main drawback to this system is its complexity. In a fixed array radar system, hundreds of phase loops would be necessary and thus the use of a modulated system becomes impractical, especially in pulsed-type radars.

Figure 3-8 shows a self-balancing phase detector for closed-loop operation.

As will be seen, the subsequent design of a phase-stabilized, helix-controlled, traveling-wave tube entails a different approach than that presented here. The two methods of closed-loop operation referred to above make use of a variable phase reference input whereas the design problem will not have the benefit of such a phase reference for correction, since phase information will be in the form of d-c helix voltages.

3.6 Conclusions

The phase detector methods are useful and may be employed in the design problem. The complexities associated with the suppressed-carrier system render it less desirable than the self-balancing system.

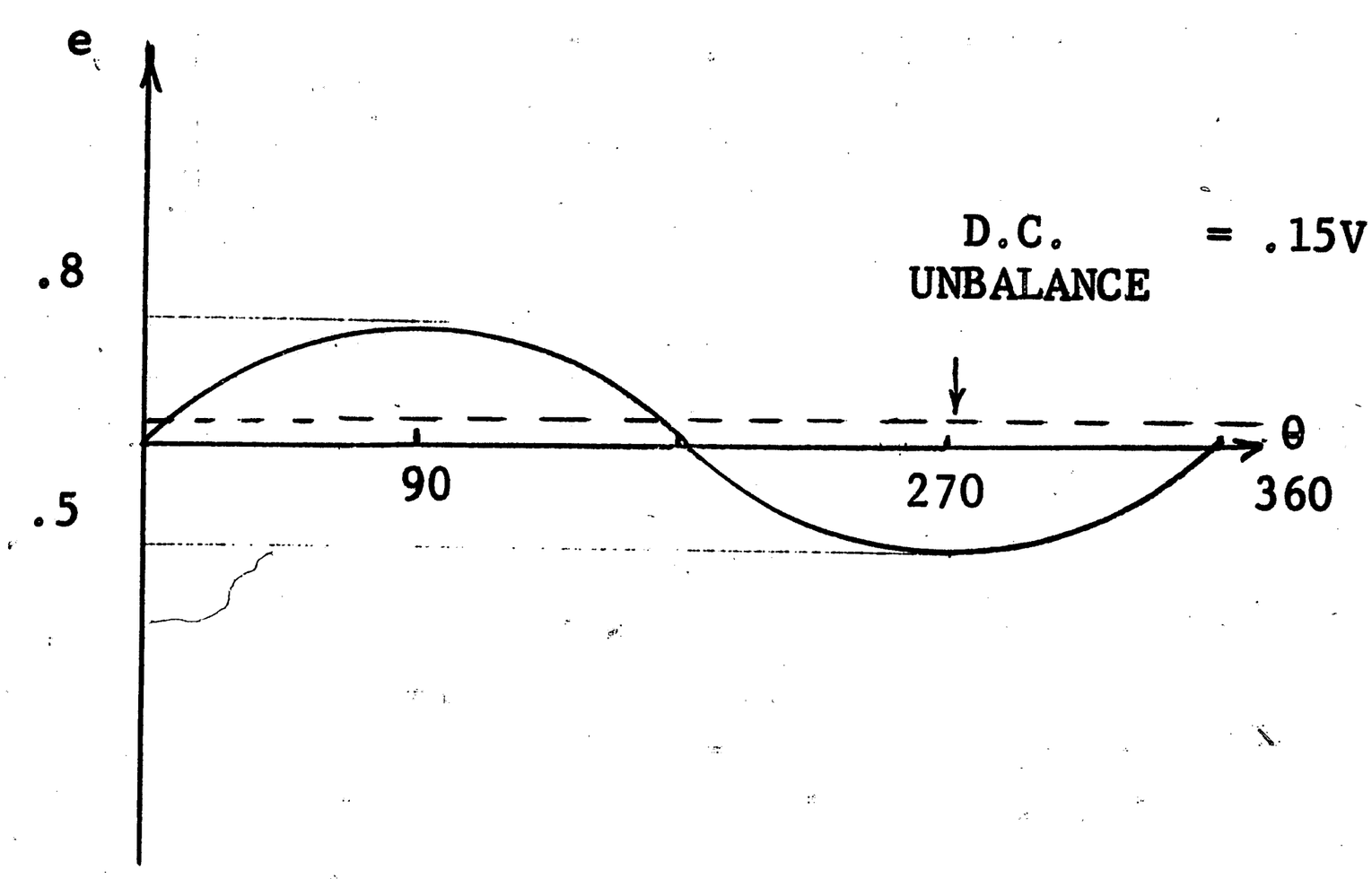

Fig. 3-6, Phase characteristics of self-balanced phase detector. (MIT)

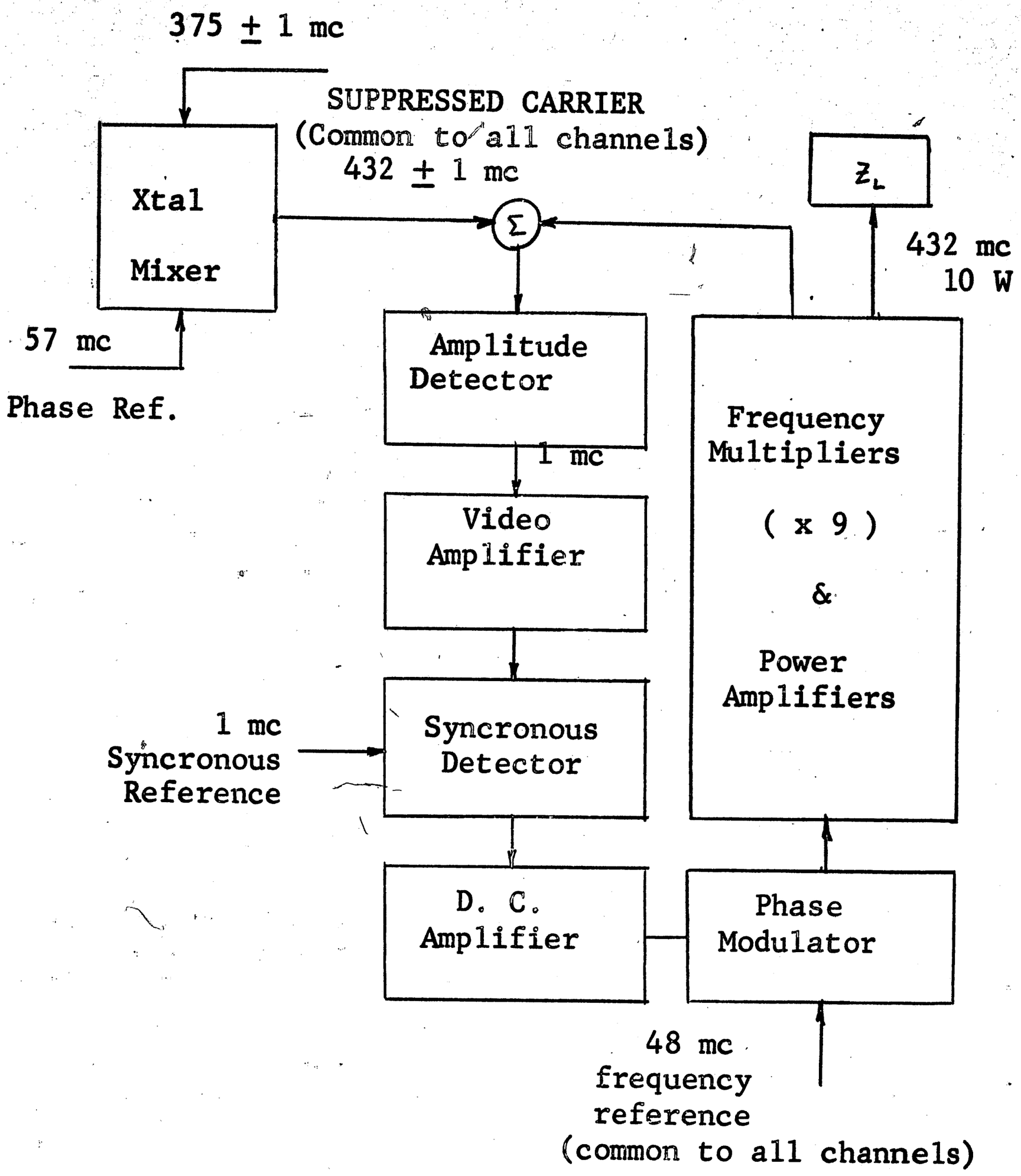

Fig. 3-7, Employment of suppressed-carrier modulated phase detector in closed-loop operation for phase stabilization. (MIT)

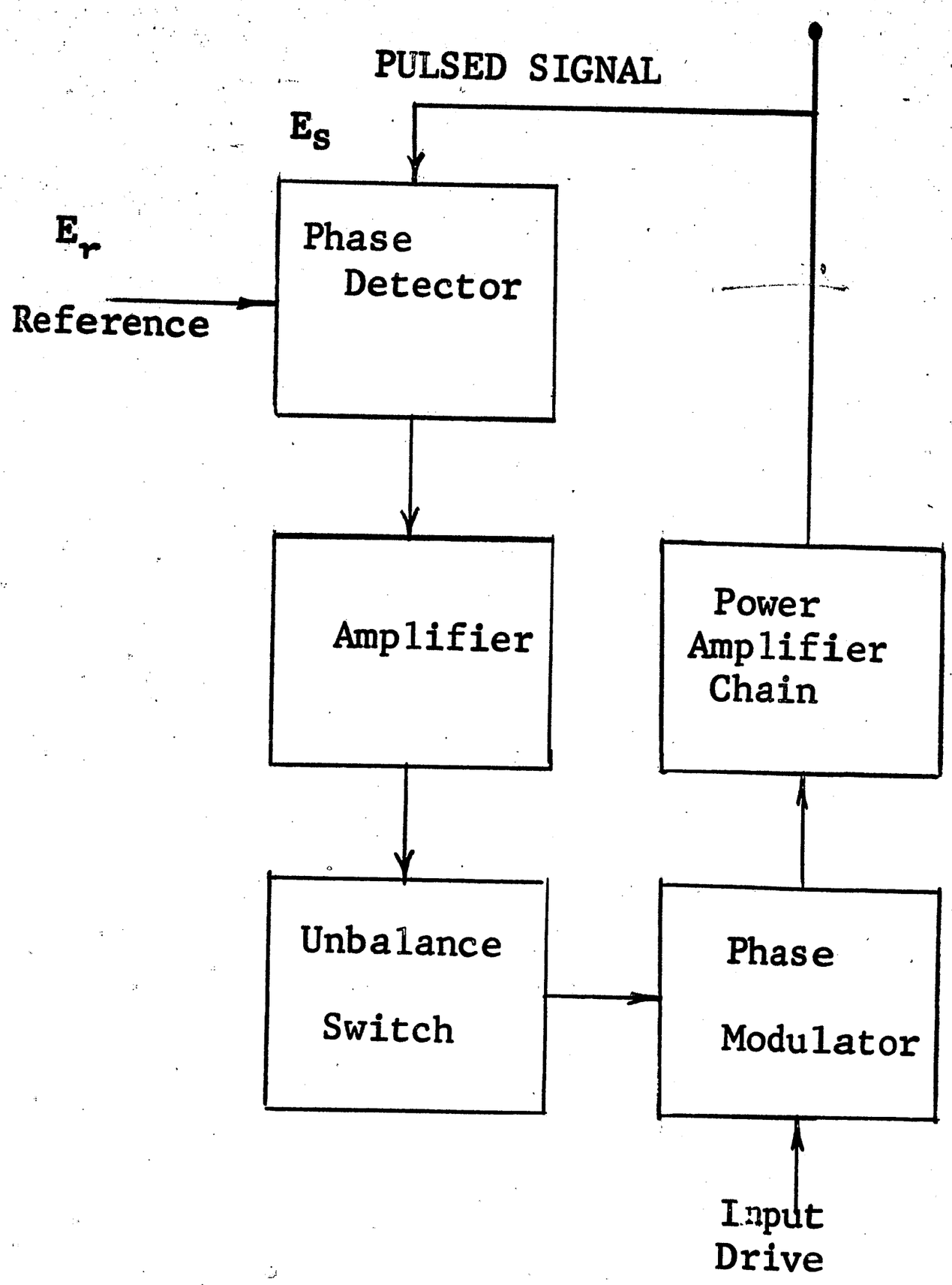

Fig. 3-8, Employment of self-balancing phase detector scheme in closed-loop operation. (MIT)

However, since the closed-loop operation presupposes a variable phase reference signal for direct control, the closed-loop methods are not useful for the specific design problem to follow, since control will be accomplished by helix voltage programming.

CHAPTER 4

DESIGN OF A PHASE-STABILIZED TRAVELING-WAVE TUBE PHASE SHIFTER

The preceding chapter described some methods of phase stabilizing traveling-wave tubes where the TWT is used as an amplifier. This concept permitted the use of a continuous closed-loop method for phase correction. However, when the traveling-wave tube is used as a phase shifter a continuous system cannot easily be incorporated since the phase of the incoming signal is constant.

This chapter deals with the design of a simple phase stabilization system for employment with a TWT used as a phase shifter.

4.1 System Requirements

To be effective, the system must be simple and free from complicated modulating and demodulating equipment since hundreds of these units would be used in a single fixed-array radar system.

The contemplated system is for pulsed radar signals where phase disturbances are sampled during the "radar-off" period—at which time information relating to the deviation from zero relative phase shift is recorded and stored. During the "radar-on" period, the stored information is presented to the helix of the traveling-wave tube and thus a phase correction is accomplished.

Specific system stipulations and assumptions are as follows:

1. Phase error measurements will be made within 5 milliseconds.
2. The system must be capable of correcting for phase disturbances within $\pm$ 180 degrees.
3. Phase disturbances are slowly varying functions of time.
4. The sampling rate will be slow in comparison to response time; thus, the system can be considered continuous.

4.2 Ambiguity and Non-Linearity Problems

A glance at the characteristics of the phase detectors already described and those to be investigated reveals sinusoidal relationships which lead to ambiguities. For example, in Figure 4-1, an output of X volts could be interpreted as a phase error of Y or Z degrees. Also from Figure 4-1, it is obvious that the phase detector is a non-linear element.

4.3 Basic Design Concepts

The design of the stabilization system must be capable of resolving the aforementioned problems and at the same time meet the requirements set forth in Section 4.1. The ambiguity problem can be solved by integrating the closed-loop error as shown in Figure 4-2. This method permits a phase error voltage to be fed back in a closed-loop correction system proportional to the area under the phase detector curve, with proper sense for elimination of the ambiguity problem.

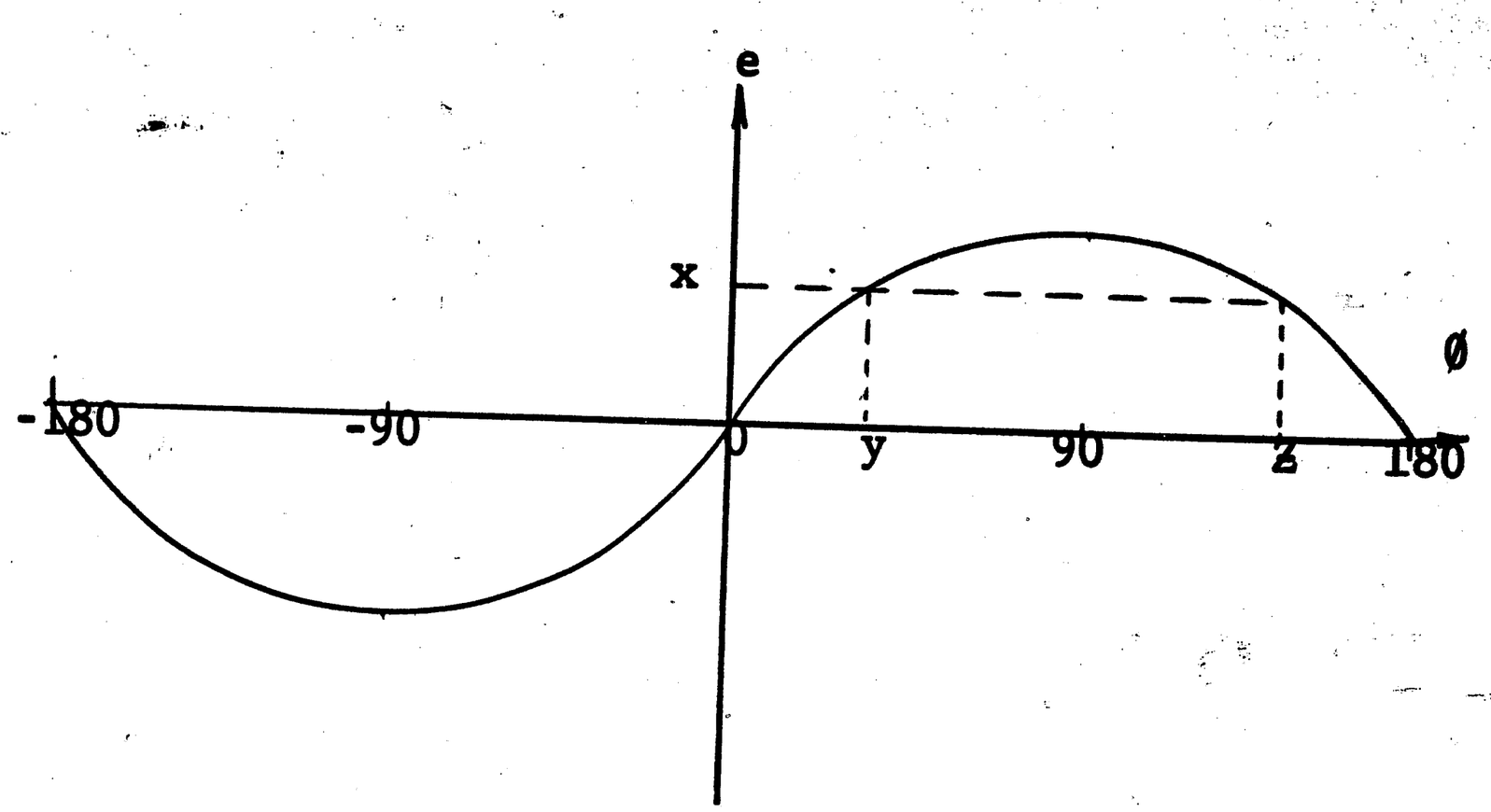

Fig. 4-1. A typical phase detector characteristic.

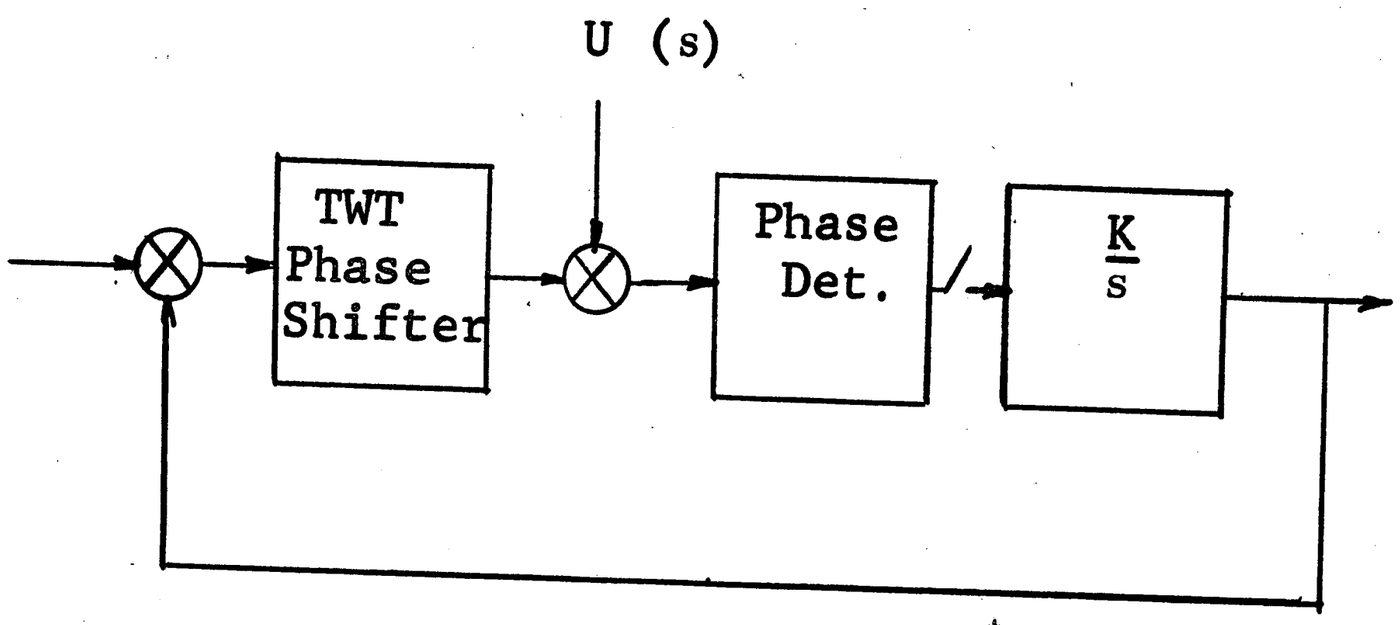

Fig. 4-2. A phase stabilization scheme employing an integrator.

As an advantage, this method also permits storage of the phase error information since the integrator output will remain although the error voltage has gone to zero. Thus the forward loop may be broken during the "radar-on" cycle and the correction voltage applied to the helix. However, since perfect operational integrators are not practically available, the design of the system and the integrator entails some limitations to be discussed in subsequent paragraphs.

Concerning non-linearity, it will suffice to say that this problem will not affect the operation of the system other than to slow down its response. The fact that the system will always correct to zero phase error can be understood by realizing that in Figure 4-1, the only stable null under closed-loop operation is at 0 degrees; other zeros are unstable. Section 4.10 will refer this topic in greater detail.

4.4 Introduction to the Analysis of Phase Detectors

In Chapter 3 a few phase detectors were described and their drawbacks with respect to the design problem mentioned. Sections 4.6, 4.7, and 4.8 are devoted to the analysis of three other phase detectors and Section 4.9 will discuss the choice of one detector for employment in the final system.

The methods are similar to the self-balancing phase detector described in Chapter 3 except that a 4-port microwave device, a coaxial hybrid, will be employed. A description and analysis of the hybrid follows.

4.5 Coaxial Hybrid

A crossover coaxial hybrid[1] is a four port device (Figure 4-3) in which each of three arms is a quarter wavelength and the fourth arm is three-quarters wavelength.

The name "crossover" arises from the fact that the three-quarter length is accomplished by reversing the wires of a quarter wavelength lead thus accomplishing an effective one-half plus one-quarter wavelength.

A signal entering port 1 divides its power equally between 2 and 4. The path length, 123, is a half wavelength and the path length, 143, is a full wavelength. Thus the split signals arrive at terminal 3, 180 degrees out of phase and cancel.

The quality of the hybrid is determined by the degree of isolation between terminals 1 and 3 and the equality of the power output at terminals 2 and 4. A hybrid of simple construction was built and tested and the results are described in the next chapter.

1. Albanese, V. J., Kagan, H., "The 'Cross-Over' Directional Coupler", The Microwave Journal, vol. 4, no. 9; September, 1961.

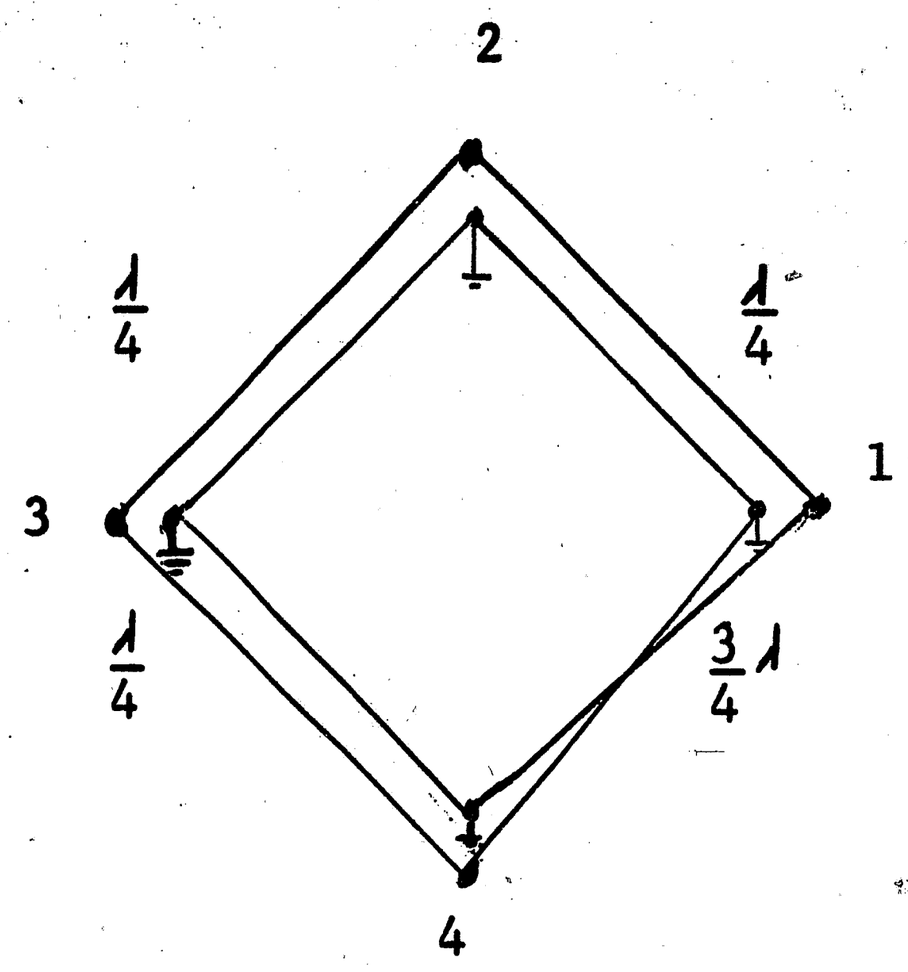

Fig. 4-3, Schematic of a coaxial hybrid.

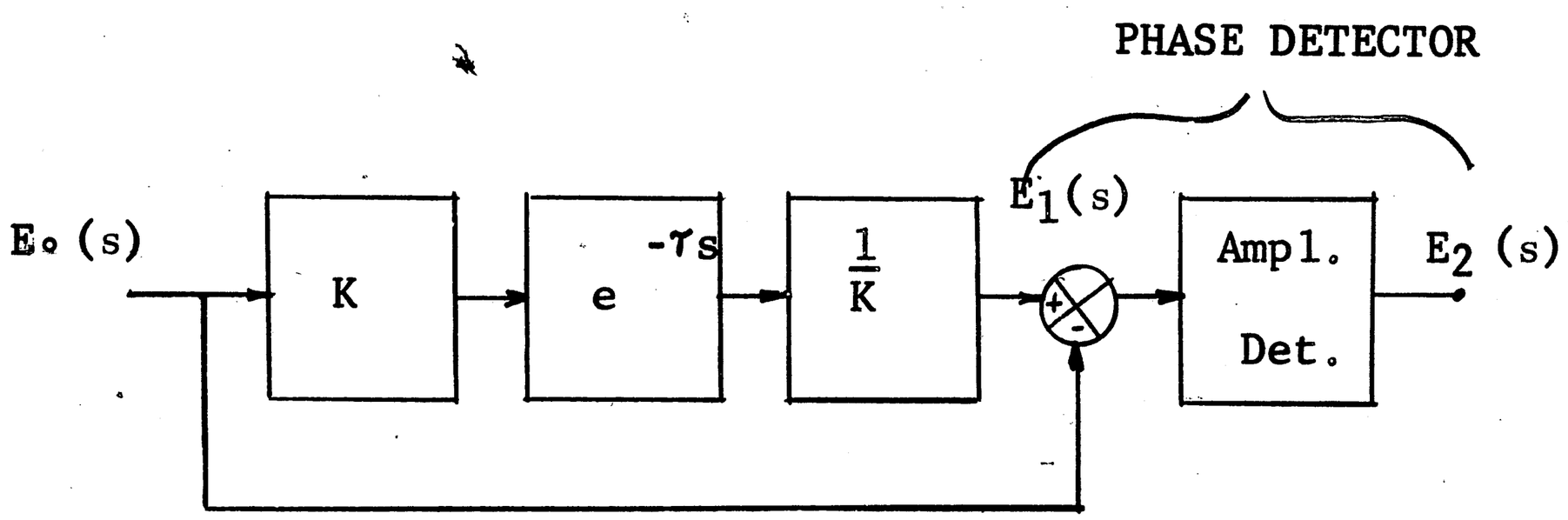

Fig. 4-4, Phase detector scheme, method 1.

4.6 Analysis of Phase Detector, Method 1

A phase detector stated as "method 1" is implied in Figure 4-4. It is similar to the Massachusetts Institute of Technology's self-balancing phase detector[1] except the comparator as shown is the above mentioned coaxial hybrid. Function $Ke^{-\tau s}$ represents the gain and phase shift of the TWT, and $\frac{1}{K}$ is an attenuator used to insure equal amplitudes at the inputs to the comparator. In this case the inputs are ports 1 and 3 of Figure 4-3 and the output is port 4 (terminal 2 is terminated). The phase characteristics are now derived by referring to Figure 4-4.

$$e_o(t) = \sin\omega t \tag{1}$$

and

$$e_1(t) = \sin(\omega t - \omega\tau). \tag{2}$$

Thus

$$e_2(t) = e_o(t) - e_1(t) \tag{3}$$

$$= \sin\omega t - \sin(\omega t - \omega\tau)$$

$$= (1 - \cos\omega\tau)\sin\omega t + \cos\omega t\sin\omega\tau. \tag{4}$$

This can be put in the form

$$e_2(t) = 1.41\sqrt{1 - \cos\omega\tau}\,\sin(\omega t + \emptyset), \tag{5}$$

where

$$\emptyset = \arcsin\left(\frac{\sin\omega\tau}{\sqrt{(1 - \cos\omega\tau)^2 + \sin^2\omega\tau}}\right) \tag{6}$$

and

$$\omega\tau = \theta = \text{phase difference}. \tag{7}$$

1. See Chapter 3.

The output of the amplitude detector is thus

$$\text{Env.} = 1.41 \sqrt{1 - \cos\omega\tau} \quad , \tag{8}$$

which is plotted in Figure 4-5 as the phase characteristic of the detector. As can be seen from the plot, proper sense cannot be obtained since only positive outputs are present. However, by the scheme of Figure 4-6 the curve can be shifted and biased to give proper sense information. The plot of the corrected curve is shown in Figure 4-8.

4.7 Analysis of Phase Detector, Method 2[1]

Method 2 also utilizes a hybrid, although in a different manner. The inputs are ports 1 and 3 while the output ports are 2 and 4 as shown in Figure 4-7. The phase characteristics will now be examined.

Let the input at 1 and 3 be e' and e'' respectively, where

$$e' = b e^{j\theta} e^{j\omega t} \tag{9}$$

$$e'' = a e^{j\omega t} = e_{in} \quad , \tag{10}$$

and θ is the relative phase difference between the two signals.

1. King, D. D., Barrack, C. M., Johnson, C. M., "Precise Control of Ferrite Phase Shifters", IRE Trans. on Microwave Theory and Techniques; April, 1959.

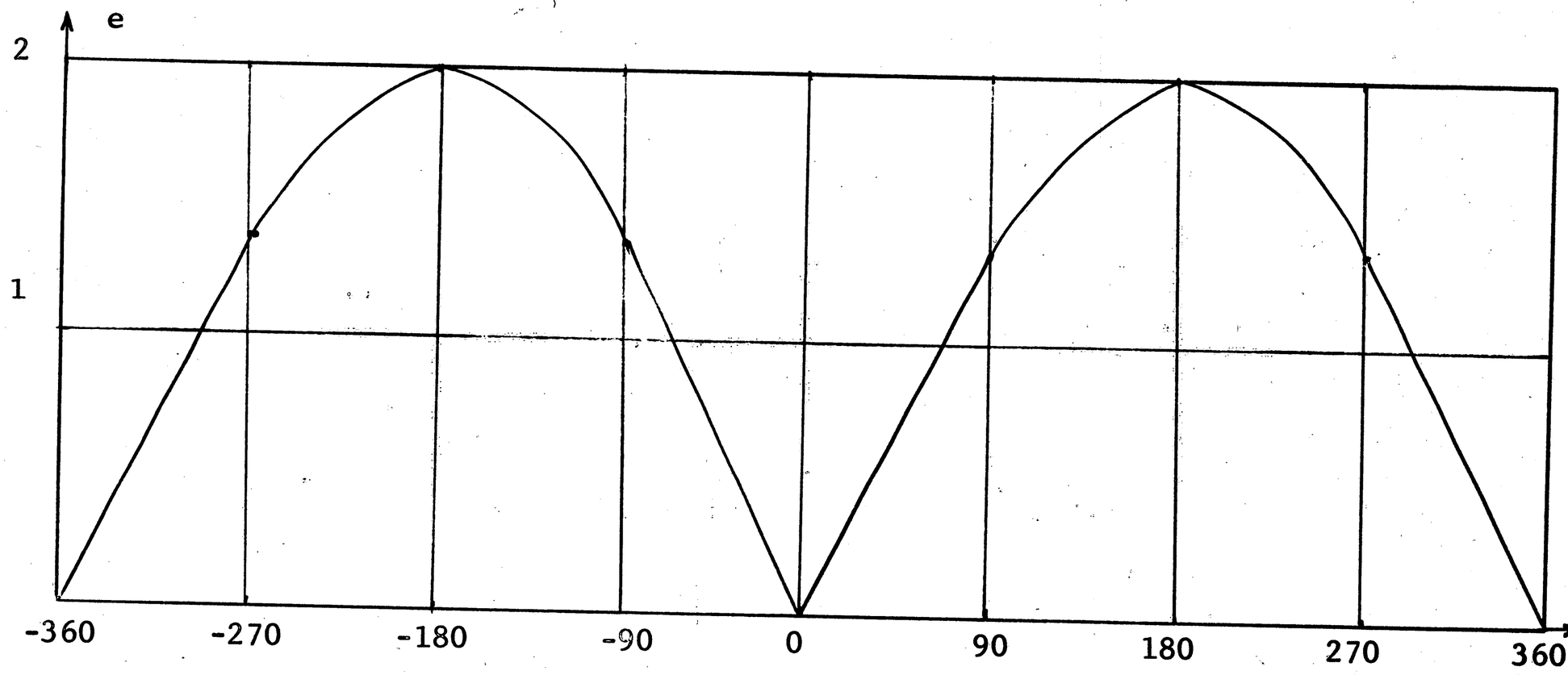

Fig. 4-5. Phase characteristics of phase detector, method 1.

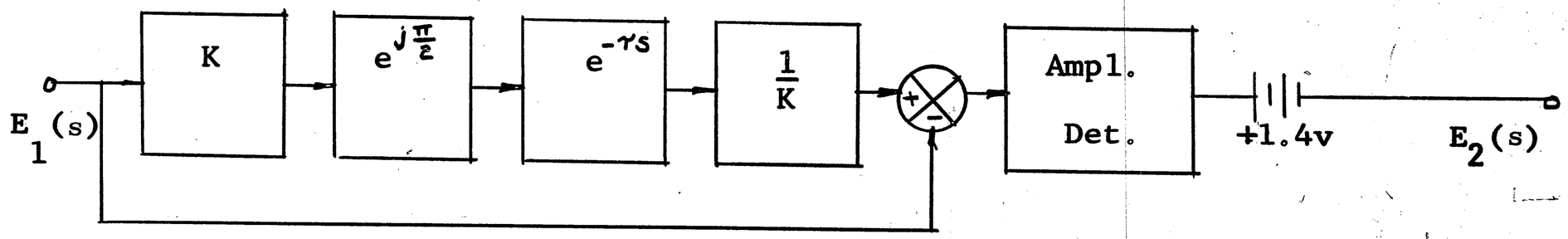

Fig. 4-6. Corrected phase detector scheme, method 1.

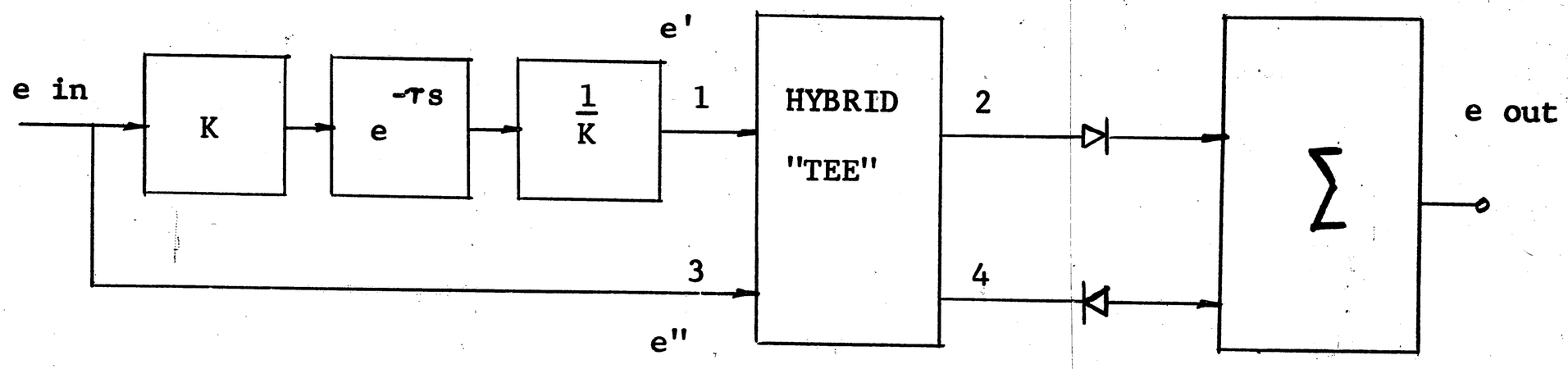

Fig. 4-7, Phase detector scheme, method 2.

The output at port 4, or A_4, is

$$A_4 = + \left[+ \frac{1}{\sqrt{2}} a - \frac{1}{\sqrt{2}} b e^{j\theta} \right] e^{j(\omega t + \frac{\pi}{2})}$$

$$= \left[1 - \frac{b}{a} e^{j\theta} \right] \frac{a}{\sqrt{2}} e^{j(\omega t + \frac{\pi}{2})} . \quad (11)$$

The output at port 2 becomes

$$A_2 = \left[\frac{1}{\sqrt{2}} a + \frac{1}{\sqrt{2}} b e^{j\theta} \right] e^{j(\omega t + \frac{\pi}{2})}$$

$$= \left[1 + \frac{b}{a} e^{j\theta} \right] \frac{a}{\sqrt{2}} e^{j(\omega t + \frac{\pi}{2})} . \quad (12)$$

The difference between $|A_2|$ and $|A_4|$ is, therefore,

$$e_{out} = |A_2| - |A_4|$$

$$= \frac{a}{\sqrt{2}} \left\{ \left(\frac{b}{a} \cos\theta + 1 \right)^2 + \left(\frac{b}{a} \sin\theta \right)^2 \right\}^{1/2}$$

$$- \frac{a}{\sqrt{2}} \left\{ \left(\frac{b}{a} \cos\theta - 1 \right)^2 + \left(\frac{b}{a} \sin\theta \right)^2 \right\}^{1/2} . \quad (13)$$

For $a = b$,

$$e_{out} = a \left(\sqrt{\cos\theta + 1} - \sqrt{1 - \cos\theta} \right) . \quad (14)$$

Thus $e_{out} = 0$ when $\theta = 90$ degrees.

It is therefore seen that this method requires a 90 degree phase correction to yield zero output for zero phase error. Also, proper sense is accomplished without the need for any bias as was the case for method 1.

The characteristics of the two methods, after biasing and shifting, are shown compared in Figure 4-8.

Before a decision is made on the type of phase detector that would be utilized in the system, it would be of interest to examine one additional possibility.

4.8 Analysis of Phase Detector, Method 3

This method employs a basic feedback loop as shown in Figure 4-9 and utilizes the same components as method 1. The results of the derivation (Appendix 4-1) are shown in Figure 4-10.

It might be added that the analysis was not carried past 1 radian since the error involved in approximating e^{-x} by the Padé approximation (see Appendix 4-1) becomes large above the 1 radian value. The plot in Figure 4-11 gives an idea of the error of the approximation.

The error in the transfer function of the closed-loop is now investigated in the light of the above paragraph.

Letting $\frac{G(s)}{K}$ equal the overall transfer function,

COMPARISON OF METHOD 1
AND METHOD 2
PHASE DETECTORS

METHOD 1

METHOD 2

Fig. 4-8

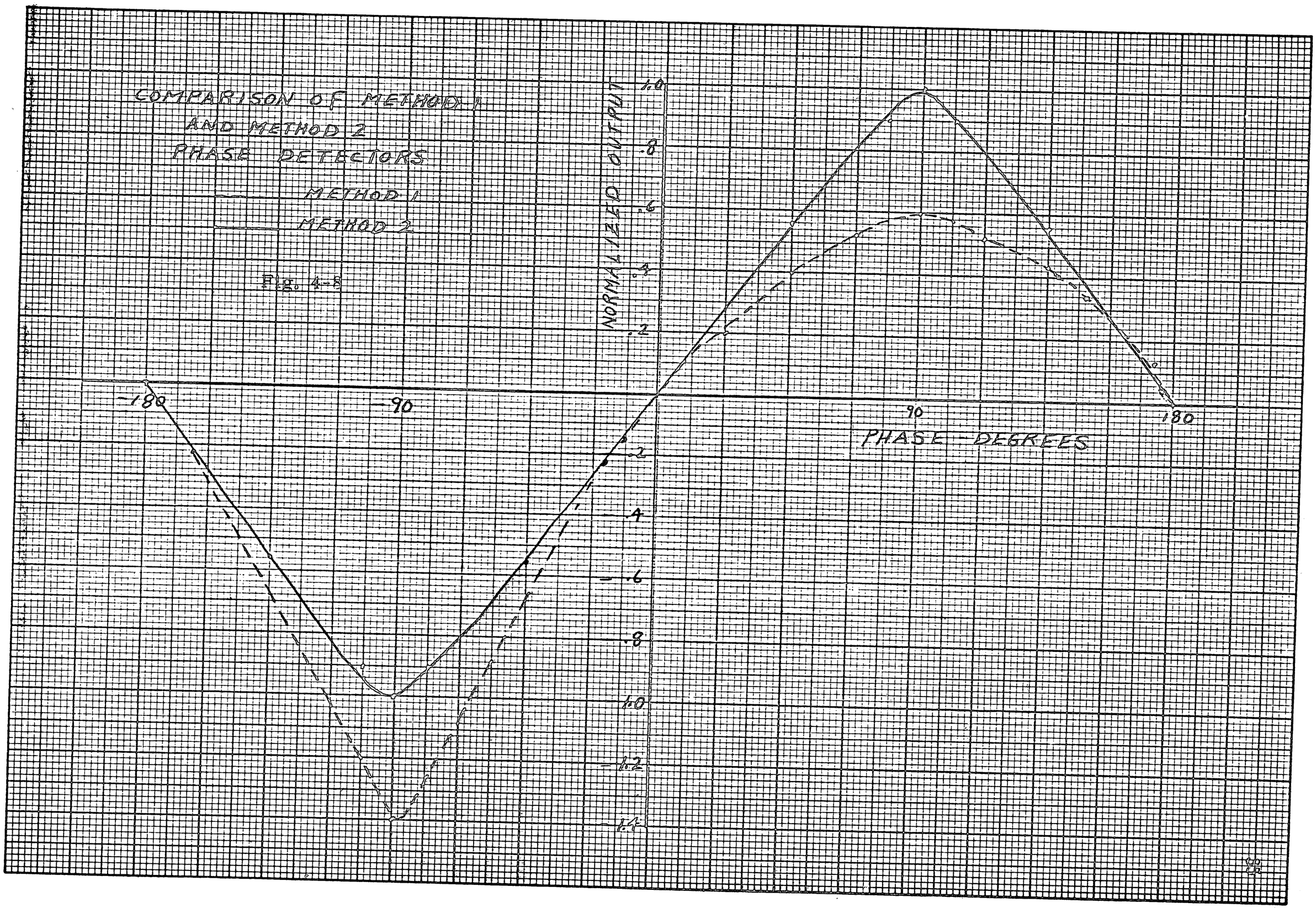

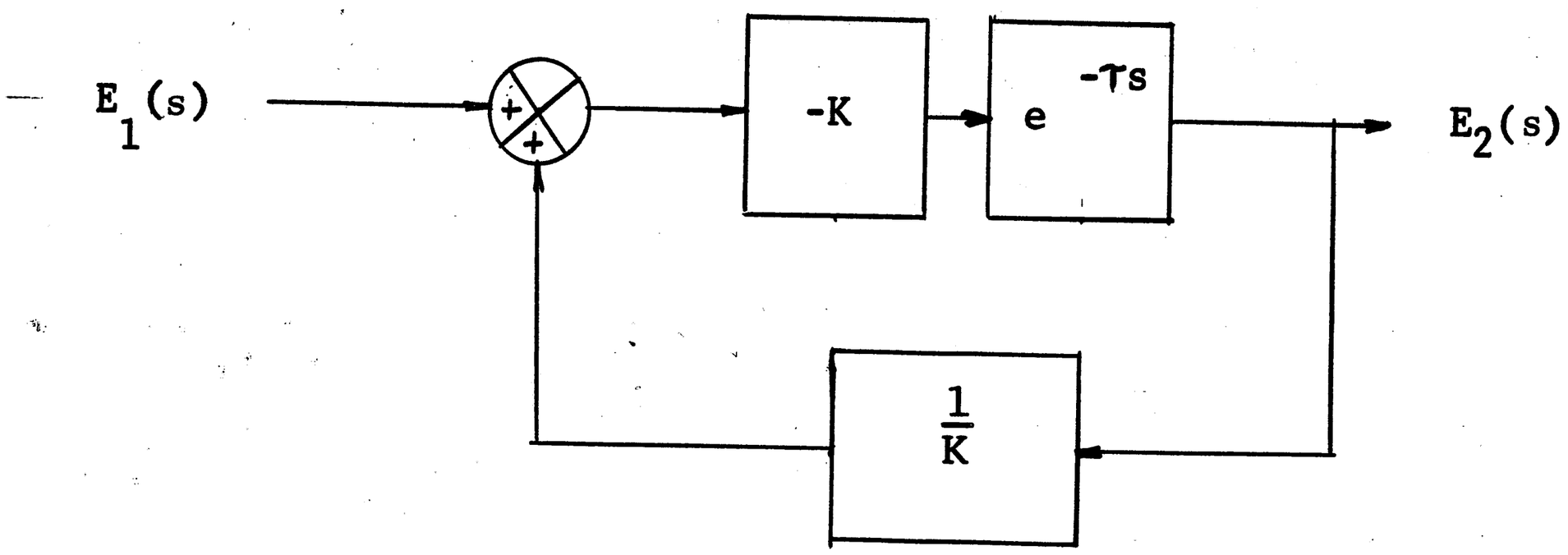

Fig. 4-9. Phase detector scheme, method 3.

PHASE CHARACTERISTICS
FOR METHOD 3 PHASE
DETECTOR

Fig. 4-10

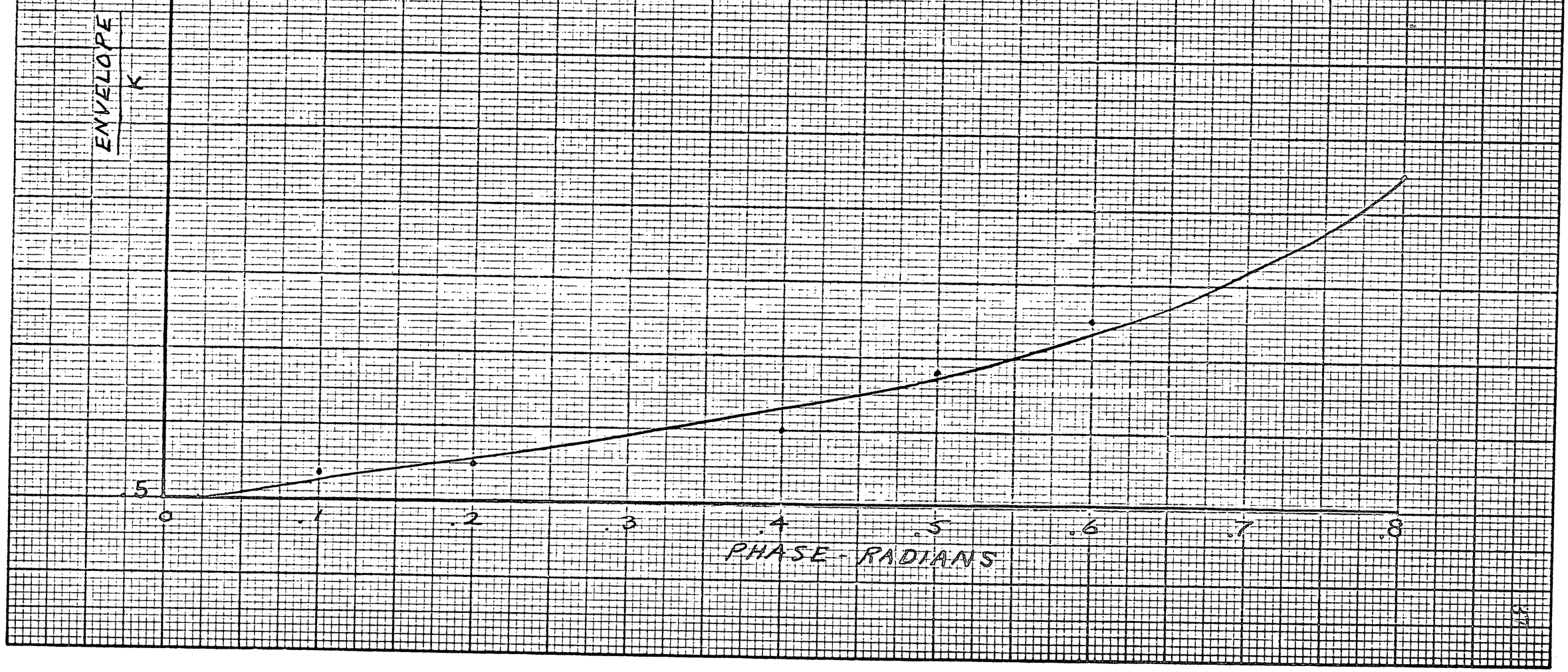

ERROR IN APPROXIMATING

e^{-x} WITH

$$\frac{1 - .33x}{1 + .67x + .456x^2}$$

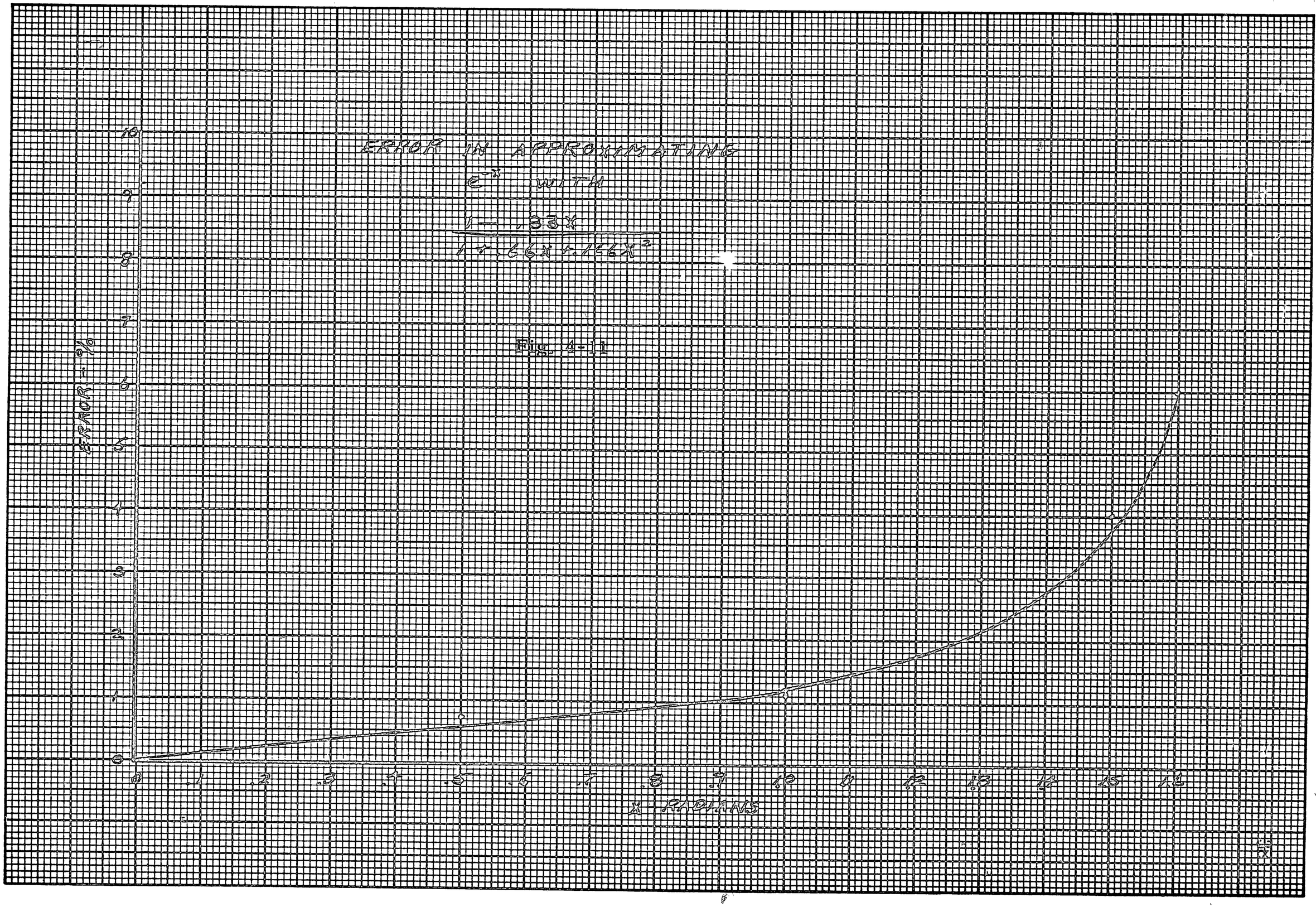

Fig. 4-11

$$\frac{G(s)}{K} = \frac{e^{-x}}{1+e^{-x}}$$

$$= \frac{1}{\frac{1}{e^{-x}} + 1} \quad , \tag{15}$$

where

$$x = \tau s \quad ,$$

Then, assuming that the error in e^{-x} is equal to a(x), the actual value used in computing the transfer function is

$$(1 + a)e^{-x} \quad . \tag{16}$$

Thus, the actual transfer function considered becomes

$$\frac{G'(s)}{K} = \frac{1}{\frac{1}{(1+a)e^{-x}} + 1}$$

$$= (1+a)\frac{1}{e^{x} + (1+a)} \quad , \tag{17}$$

yielding the error in the final result

$$\frac{G(s) - G'(s)}{G(s)} = 1 - \frac{(1+a)(e^{x}+1)}{e^{x}+1+a} \quad . \tag{18}$$

It can be shown that this error approximates the error involved in the approximation of e^{-x}.

4.9 Conclusions on the Use of a Phase Detector

Method 2 affords the most likely prospect for a phase detecting device since, unlike method 1 which is unbalanced around the θ axis, method 2 will give the same response time for both negative and positive phase errors. Also, method 2 will not entail the use of an added bias supply.

The limited analysis of method 3 indicates the need for an added bias supply, since an examination of the envelope shows that negative voltages will not appear and thus, without bias, phase sense is lost. For small values of phase error, method 3 also affords little sensitivity as can be seen from the flatness of the characteristic curve.

4.10 System Stability

The basic system to be used is shown in Figure 4-12. The design criteria imposed on the integrator will be discussed following an examination of system stability.

The characteristic equation of the system is

$$s - K_1 K_2(\theta) K_3 = 0 \ , \tag{19}$$

where

K_1 = phase sensitivity of TWT,

$K_2(\theta)$ = phase characteristics of the phase detector,

and K_3 = gain of integrator.

The non-linearity of the phase detector will entail a slight alteration whereby the discussion of stability will be broken into two parts:

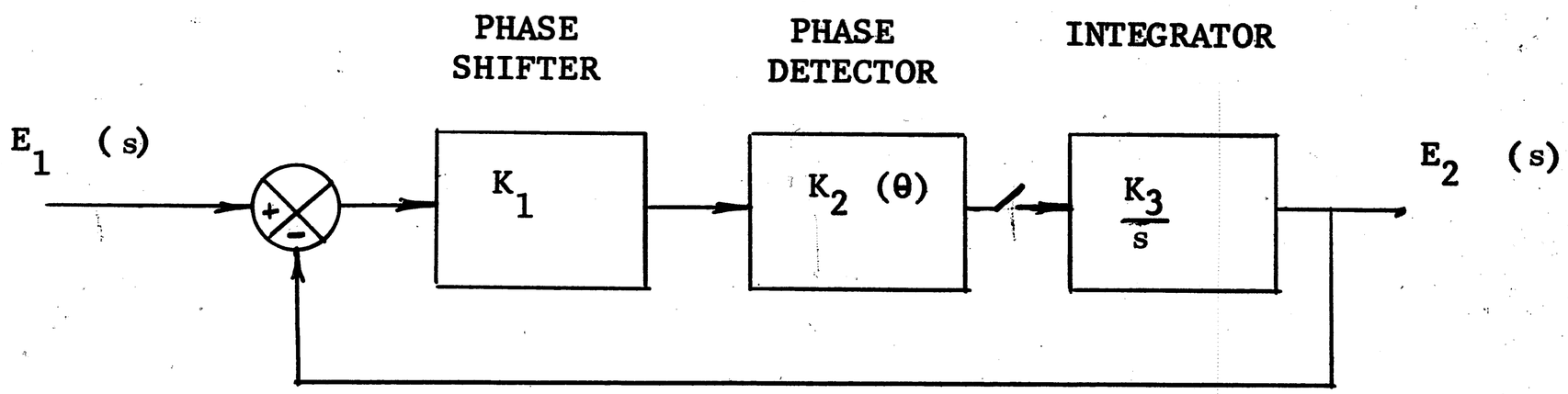

Fig. 4-12. Phase stabilization system.

(a) phase errors between ± 90 degrees

(b) phase errors outside of ± 90 degrees.

For phase errors between ± 90 degrees,

K_1 is always negative,

K_2 is positive or negative,

and K_3 is always negative.

Thus, for stability, K_2 must be negative.

This can be accomplished by proper location of the forward and reversed diode detectors at the output ports of the hybrid. For phase errors greater than $|90^\circ|$ and the approximation that the curve of Figure 4-8 (method 2) is triangular, these errors will cause instability since $K(\theta)$ is positive. However, the correction is in the direction to drive the error to zero. Thus when the phase detector voltage approaches peak voltage, $K(\theta)$ becomes negative and we have the previous case, clarifying the statement that "zero degree" is a stable null while the adjacent zeros are unstable nulls.

4.11 Integrator Constraints

An equivalent circuit of an operational integrator is shown in Figure 4-13 along with a square wave input and the corresponding output. A characteristic of a perfect integrator ($A = \infty$) is that after integration the device will hold the final value as shown. This phenomenon will be used as a memory for the phase stabilization system as previously explained.

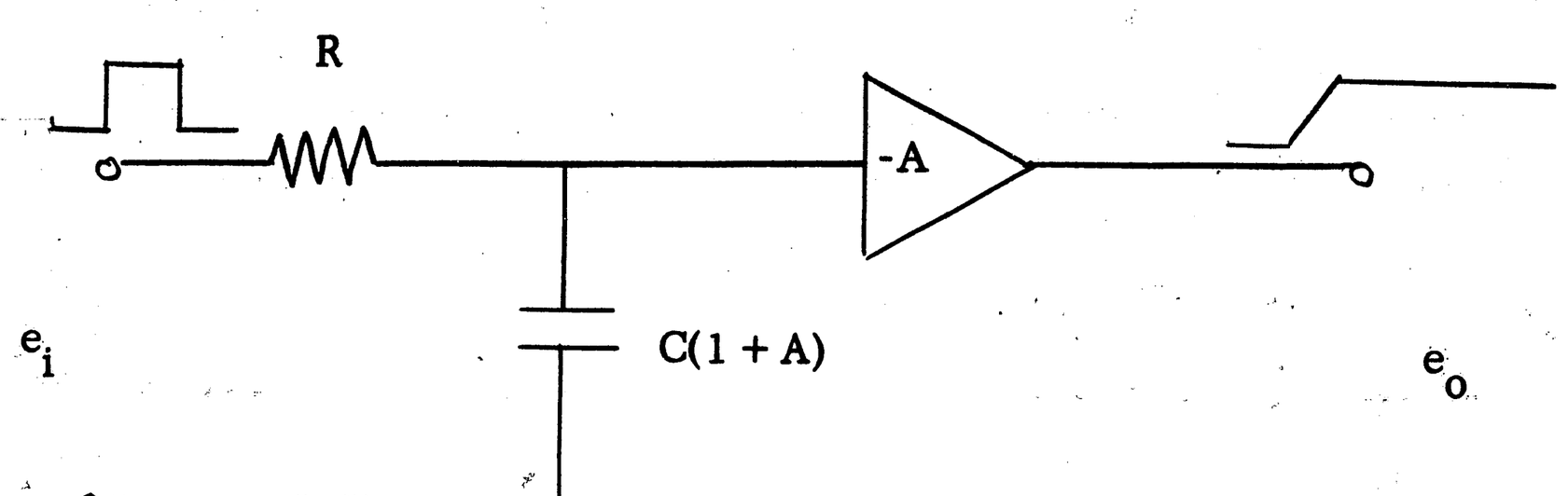

Fig. 4-13. Equivalent circuit of an operational integrator.

If A does not equal infinity, then a decay of the final value will take place as a function of time if the integrator input is grounded after the error goes to zero. It is this unwanted decay that will force certain constraints on integrator parameters so that a commercially available integrator can be used.

In Figure 4-13

$$\frac{e_o}{e_i} = \frac{-A}{RC(1+A)s+1}$$

$$= \frac{-\frac{A}{1+A}}{RC\left(s+\frac{1}{RC(1+A)}\right)} \quad . \tag{20}$$

The decay term,

$$e^{\frac{1}{-RC(1+A)}t} \approx e^{\frac{1}{-RCA}t} \tag{21}$$

is a measure of how well the output will hold its final value after application of a test square wave to the input.

For the output to be, say, within 1 % of its final value

$$\frac{1}{RCA}t = .01, \tag{22}$$

and to be within this tolerance for 10 seconds (sampling time estimate)

$$RCA = 1000. \tag{23}$$

In general, for small voltage tolerances,

$$\frac{1}{RCA} = \frac{\text{voltage tolerance permissible}}{\text{time desired for near perfect operation}} , \qquad (24)$$

since,

$$e^{\pm x} \approx 1 \pm x \qquad (25)$$

for small x.

For an operational amplifier with a gain of 10^7, equation (24) yields a minimum RC, of 10^{-4}.

4.12 Design for Response Time

As stated at the beginning of this chapter the system must correct for any phase errors within 5 milliseconds.

Considering the characteristic equation

$$s + K_1K_2K_3 = 0 , \qquad (26)$$

where

K_1 = phase sensitivity of TWT helix

$$\approx - \frac{\pi \text{ rad.}}{40 \text{ v}}$$

$$= - .075 \text{ rad/v} ,$$

$$K_2 = - \frac{\sqrt{2}\, a\, K'}{\frac{\pi}{2}} \text{ v/rad}$$

$$= - .9\, a\, K' ,$$

$$K_3 = -\frac{1}{RC} ;$$

and

a = amplitude of rf at hybrid input,

K' = gain of adder,

RC = product of integrator components;

the response time is given by

$$T_R = 3\left(\frac{1}{K}\right)^{*} \tag{27}$$

$$= 3\left(\frac{RC}{.07\, a\, K'}\right)$$

$$\approx 45\,\frac{RC}{a\,K'}\,, \tag{28}$$

where K = total loop gain = $K_1K_2K_3$.

In this only errors to $\left|90^{o}\right|$ were considered.

For errors outside of $\left|90^{o}\right|$ the characteristic equation is,

$$s - K_1K_2K_3 = 0 \tag{29}$$

assuming the characteristics of the phase detector of Figure 4-8 can be represented as triangular.

Now, assume an input error of Q volts representing nearly 180 degrees phase error is present. Then the output of the integrator is the same as a

* Gille, J. C., Pelegrin, M. J., Decaulne, P., "Feedback Control Systems", McGraw-Hill, New York, pp. 70-71; 1959.

case where K_2 is positive and an input error voltage of $-\underline{E}'$ is applied at the helix. Here,

$Q + E'$ = voltage representing 180^o phase error at helix.

Thus, for an input error voltage, Q,

$$E_o(s) = \left(\frac{-E'}{s}\right)\left(\frac{K}{s-K}\right) = E'\left(\frac{1}{s} - \frac{1}{s-K}\right), \qquad (30)$$

where, after application of the inverse Laplace transformation yields,

$$e_o(t) = E'(1 - e^{Kt}). \qquad (31)$$

For the system to become stable,

$$e_o(t) = -\frac{Q+E'}{2} \quad . \qquad (32)$$

That is, the system will have corrected the error outside of $|90^o|$ and K_2 will change sign thus making the system stable.

The time for this is found as follows:

$$e_o(t) = -\frac{Q+E'}{2} = E'(1 - e^{Kt}); \qquad (33)$$

therefore,

$$t = \frac{Ln\,(3 + \frac{Q}{E'}) - Ln\,2}{K}$$

$$= \frac{Ln\,(3 + \frac{Q}{E'}) - 0.7}{K} \qquad (34)$$

Thus the total response time of the system for errors of approximately $|180^o|$ is

$$T_R = \frac{2.3 + Ln\,(3 + \frac{Q}{E'})}{K} \qquad (35)$$

As an example, for an error of $\approx 180^{o}$, a loop gain of 3500, and $K_1 = 40$ v/π rad.

$$T_R \approx \frac{2.3 + \text{Ln}\ (3 + \frac{39.9}{0.1}\ )}{3500} = 0.0024 \text{ sec.}$$

4.13 Conclusions

Three types of phase detectors were investigated and method 2 was chosen for incorporation in the final system. This chapter leads to the following criteria regarding a particular type of phase stabilization system:

(a) $\frac{1}{RCA} = \frac{\text{voltage tolerance permissible}}{\text{time desired for near perfect operation}}$, (36)

(b) K_2 must be negative for stability, (37)

(c) $\frac{3}{K}$ = response time for errors less than $\left|90^{o}\right|$, (38)

(d) $\frac{2.3 + \text{Ln}\ (3 + \frac{Q}{E'})}{K}$ = response time for errors of approximately $\left|180^{o}\right|$, (39)

where

RCA = product of integrator gain and components,

K_2 = phase detector gain,

K = total loop gain,

$Q + E'$ = voltage representing $\left|180^{o}\right|$ phase error at helix,

Q = voltage representing a phase error of approximately $\left|180^{o}\right|$.

The next chapter will describe some experimental results obtained in the laboratory for a system specifically set up to meet the requirements of Section 4.1.

CHAPTER 5

LABORATORY TEST OF THE PHASE STABILIZATION SYSTEM

This chapter describes the experimental results obtained from the phase stabilization system covered in the last chapter.

Sections 5.1 and 5.2 deal with the characteristics of system components, in order that observed phenomena can be understood adequately. Subsequent sections will describe the characteristics of the system itself.

5.1 Coaxial Hybrid Characteristics

Power split and isolation were mentioned before as measures of the operation of a coaxial hybrid. Figures 5-1 and 5-2, respectively, describe these results for a hybrid of simple construction built in the laboratory following the theory of Section 4.5.

The best frequency for trade-off with respect to power split for the two input terminals is about 1625 kilomegacycles yielding a maximum difference of 0.5 db between the two output terminals. For this frequency, the isolation is seen to be comparable to commercial units, or about 25 db.

POWER SPLIT CHARACTERISTICS OF COAXIAL HYBRID (OUTPUT TERM. #2 & 4)

Fig. 5-1

INPUT TERM. 3

INPUT TERM. 1

OUTPUT TERM. 2

OUTPUT TERM. 4

A POWER-DB

1.0
.9
.8
.7
.6
.5
.4
.3
.2
.1
0

1100 1200 1300 1400 1500 1600 1700 1800 1900

FREQUENCY - MC.

ISOLATION CHARACTERISTICS FOR COAXIAL HYBRID (INPUT TERM. #1 OUTPUT TERM. #3)

Fig. 2

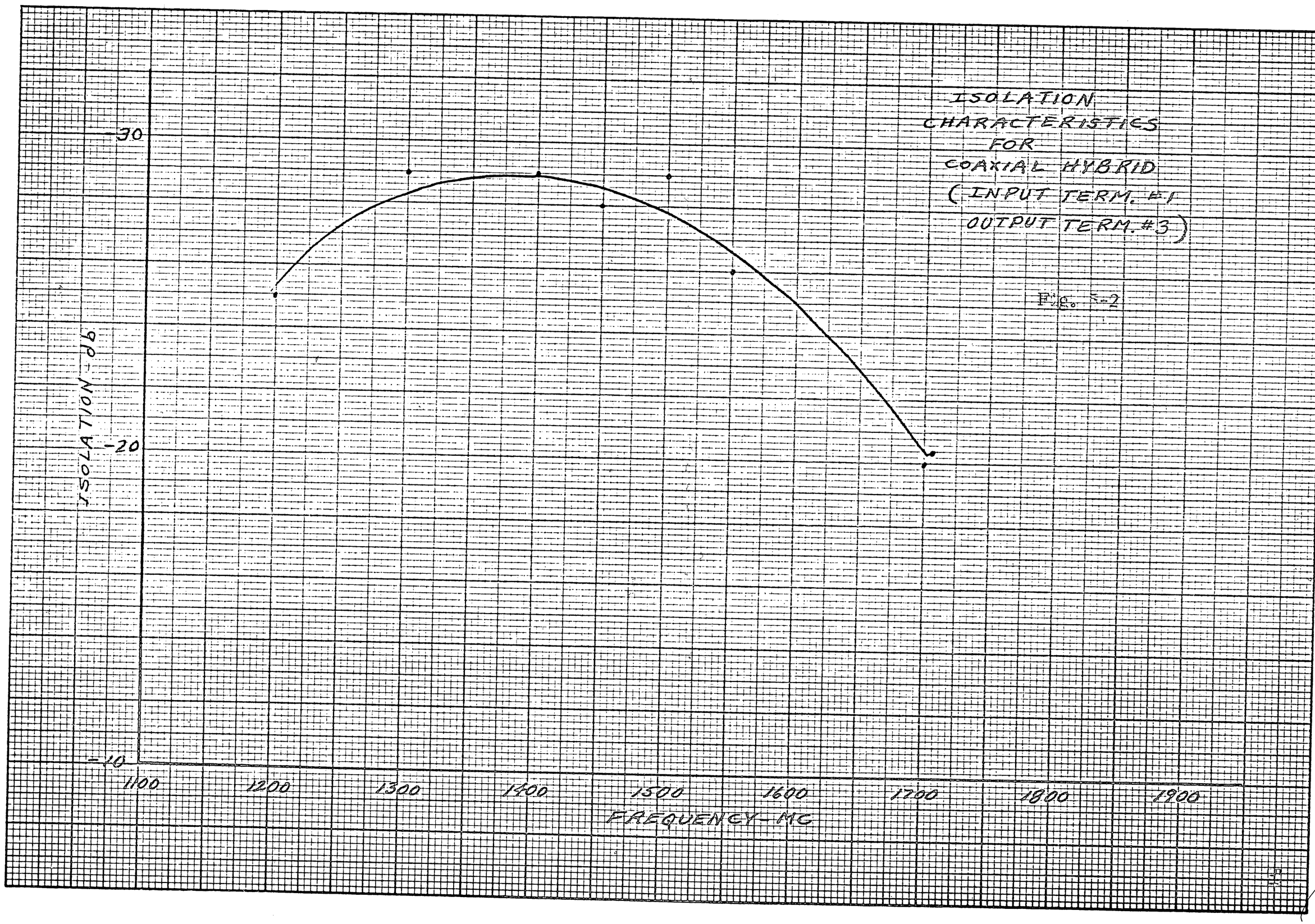

VSWR CHARACTERISTICS
FOR COAXIAL
HYBRID

Fig. 5-3

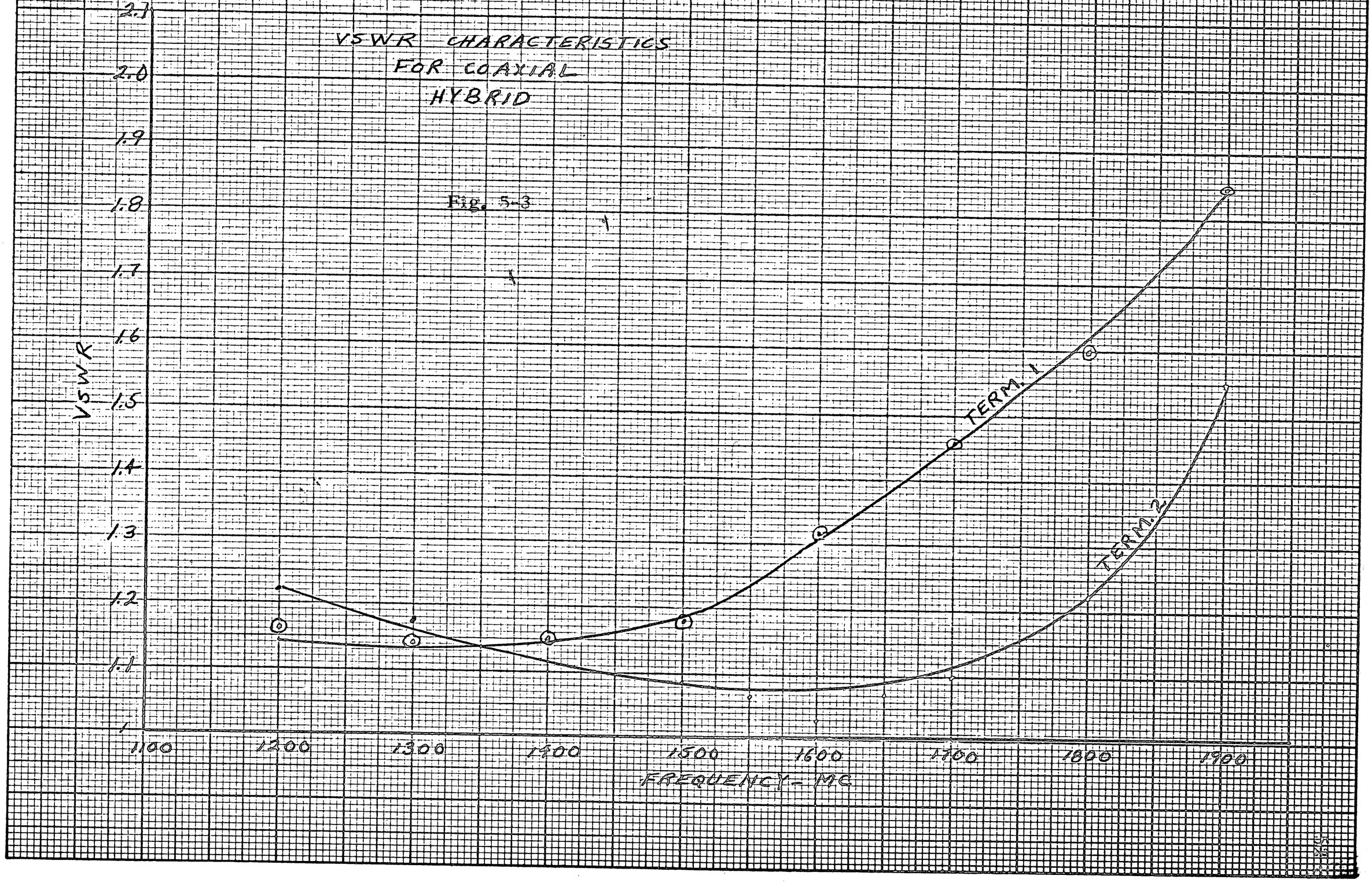

Figure 5-3 demonstrates the VSWR-frequency characteristics for selected input and output terminals of the hybrid where, for 1625 kmc, the maximum VSWR is 1.35. Again, this figure agrees favorably with hybrid units on the market.

5.2 Phase Detector Characteristics

The normalized phase detector characteristic, shown in Figure 5-4, reveals more flatness around ± 90 degrees than the derived characteristic of Figure 4-8 (method 2). Thus, it is expected that for errors larger than 45 degrees, the system response time will not be as short as that derived analytically.

5.3 Laboratory Test of the Phase Stabilization System

The system was tested under the conditions of the diagram of Figure 5-5 with the list of major equipment itemized in Figure 5-6.

TWT (2) is the traveling-wave tube whose phase is being stabilized and whose helix voltage-phase characteristic is shown in Figure 5-7.

TWT (1) is used to amplify the oscillator output.

Function $\frac{1}{K_{ps}}$ arises from the fact that the use of resistive adding networks in the helix supply cuts the loop gain down by 1/3, a value which agrees with .34, the measured transfer from the integrator to the helix.

EXPERIMENTAL
PHASE DETECTOR
— CHARACTERISTICS

Fig. 5-4

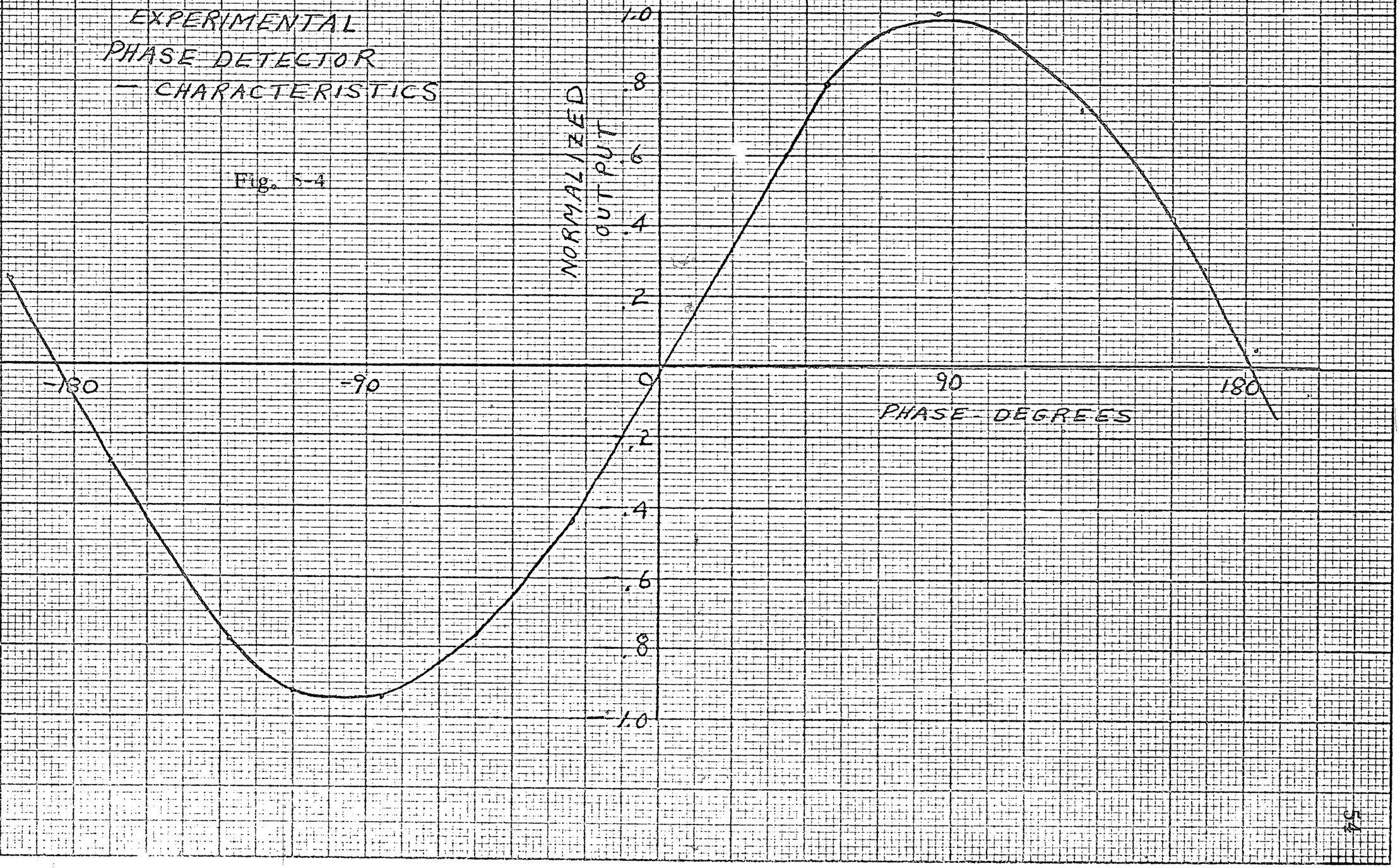

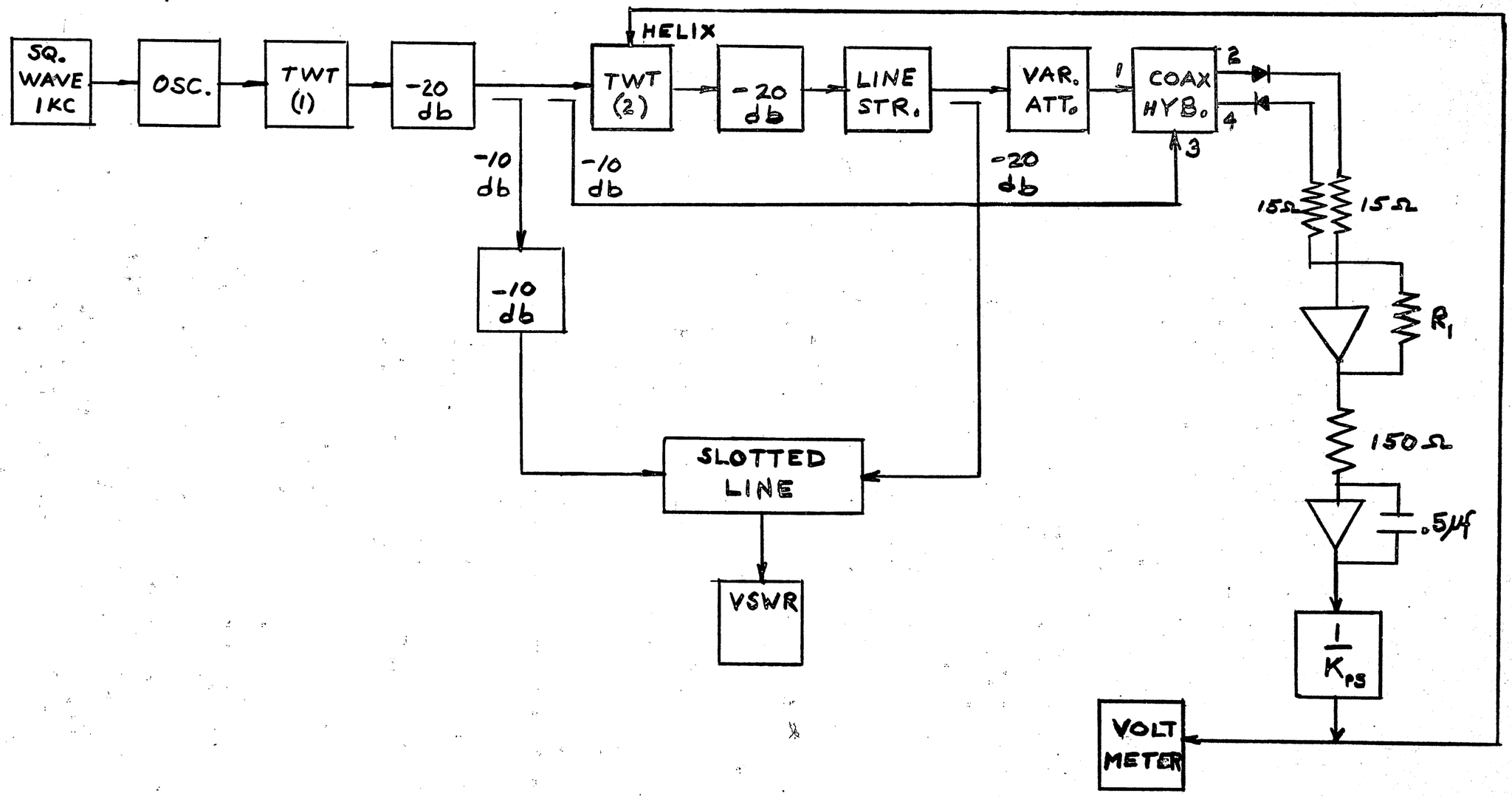

Fig. 5-5. Laboratory test of phase stabilization system. TWT (2) is shown being corrected by the feedback loop.

MAJOR COMPONENTS USED IN LABORATORY TEST OF PHASE STABILIZATION SYSTEM

TWT (1) and (2) - Sylvania 6752

Operational adder and integrator - Philbrick USA-3 (gain = 10^7)

Diodes - Microwave Associates, MA421B, MA421BR

Adjustable line length - General Radio 10 cm line

Variable attenuator - Arra π Line 1414-10

Voltmeter - Kintel 301

Padded crystal mounts - Microlab XP-1040

Fig. 5-6

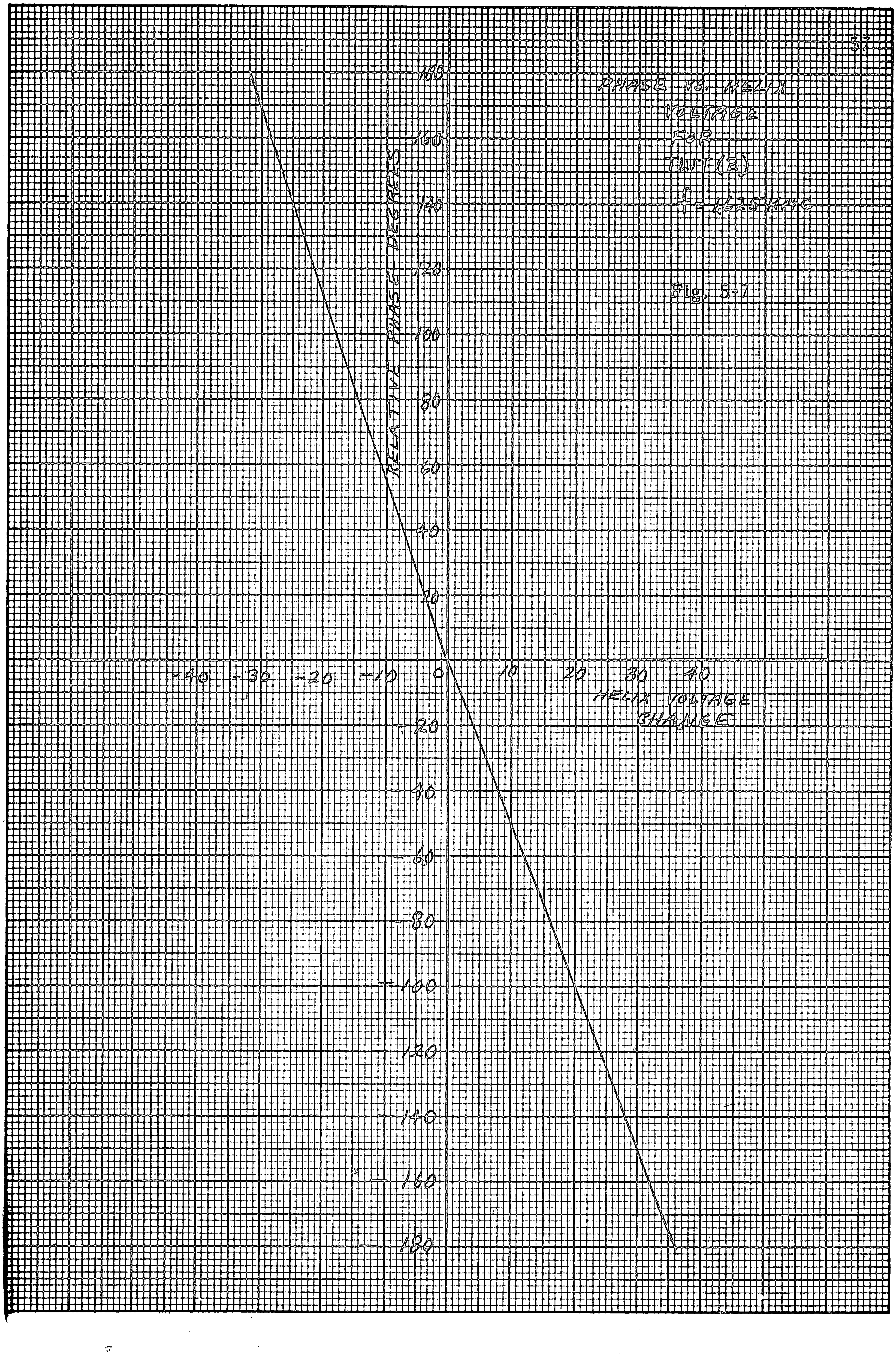
PHASE VS. HELIX
VOLTAGE
FOR
TWT(2)
RELATIVE PHASE DEGREES
180
160
140
120
100
80
60
40
20
0
20
40
60
80
100
120
140
160
180
-40
-30
-20
-10
10
20
30
40
HELIX VOLTAGE
CHANGE

Fig. 5-7

The variable attenuator was used to balance the input-signal amplitude to the coaxial hybrid while the adjustable line length introduced the 90 degree phase shift required for reasons discussed in Section 4.7

The use of the remaining equipment will become clear as each test is described in subsequent paragraphs.

5.4 Response Time

In order to measure the response time of the system a square wave with sufficient amplitude to cause a 25 degree phase error was introduced at the input to the integrator as shown in Figure 5-8.

The response time was measured over a usable range of gain.[1] The values are summarized in Figure 5-9 for both the positive and negative slope and are seen to fall within the 5 millisecond design. Also, the theoretical values for response time are included and demonstrate the agreement between the experimental and theoretical results. Figure 5-10 shows a system response of 1 millisecond for a gain of 3500 and an error of 25 degrees.

1. The method for determining loop gain is demonstrated in Appendix 5-1. Also, gains above 3500 produced damped oscillations and gains below 600 produced response times which were too slow to meet the design requirements. Increased response times were limited by the gain and rise time characteristics of the operational amplifiers at higher frequencies.

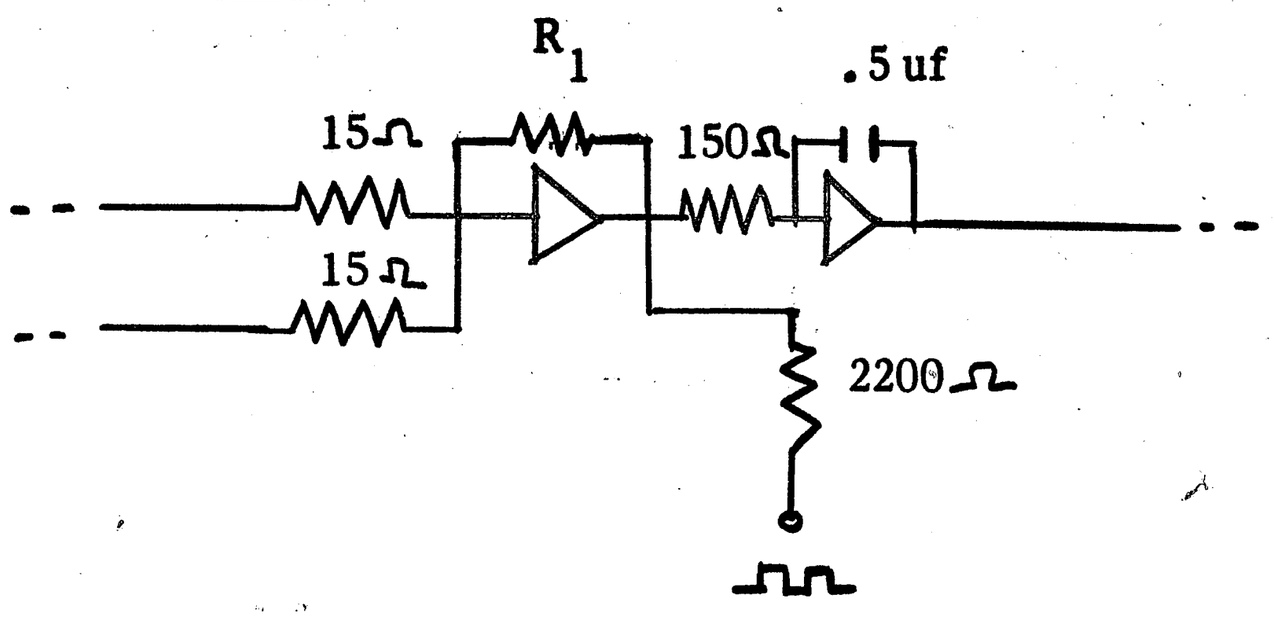

Fig. 5-8 Application of a square wave error to the phase stabilization system.

Gain	T_{R_+}	T_{R_-}	Theoretical T_R Eq. (4-27)
3500	1.0 ms	0.8 ms	0.855 ms
1750	1.6 ms	1.5 ms	1.710 ms
685	5.0 ms	4.5 ms	4.390 ms

Fig. 5-9 Table of response times for various values of loop gain with the introduction of a 25° error.

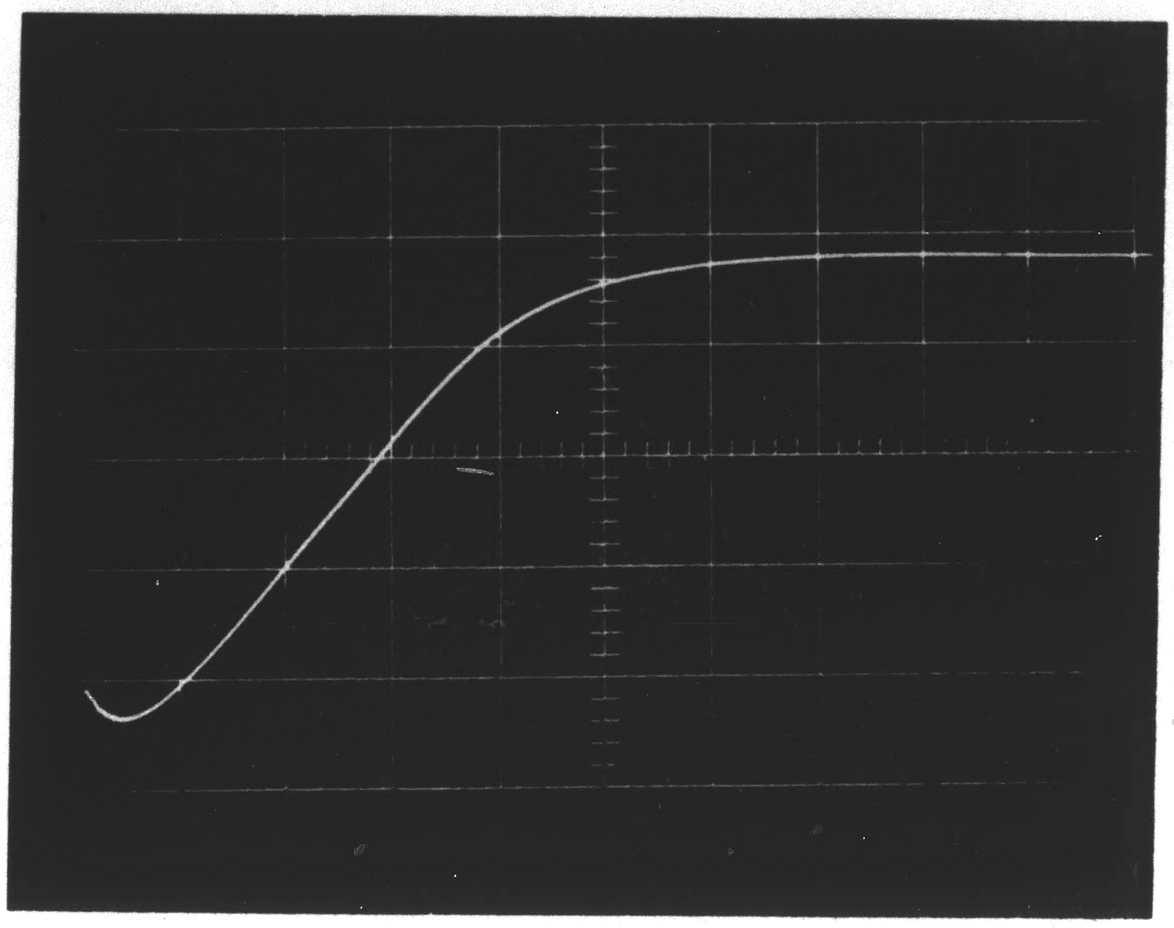

Fig. 5-10. Response of phase stabilization system at the helix for a loop gain of 3500 (error = 25°, 200 us/cm, 1 v/cm).

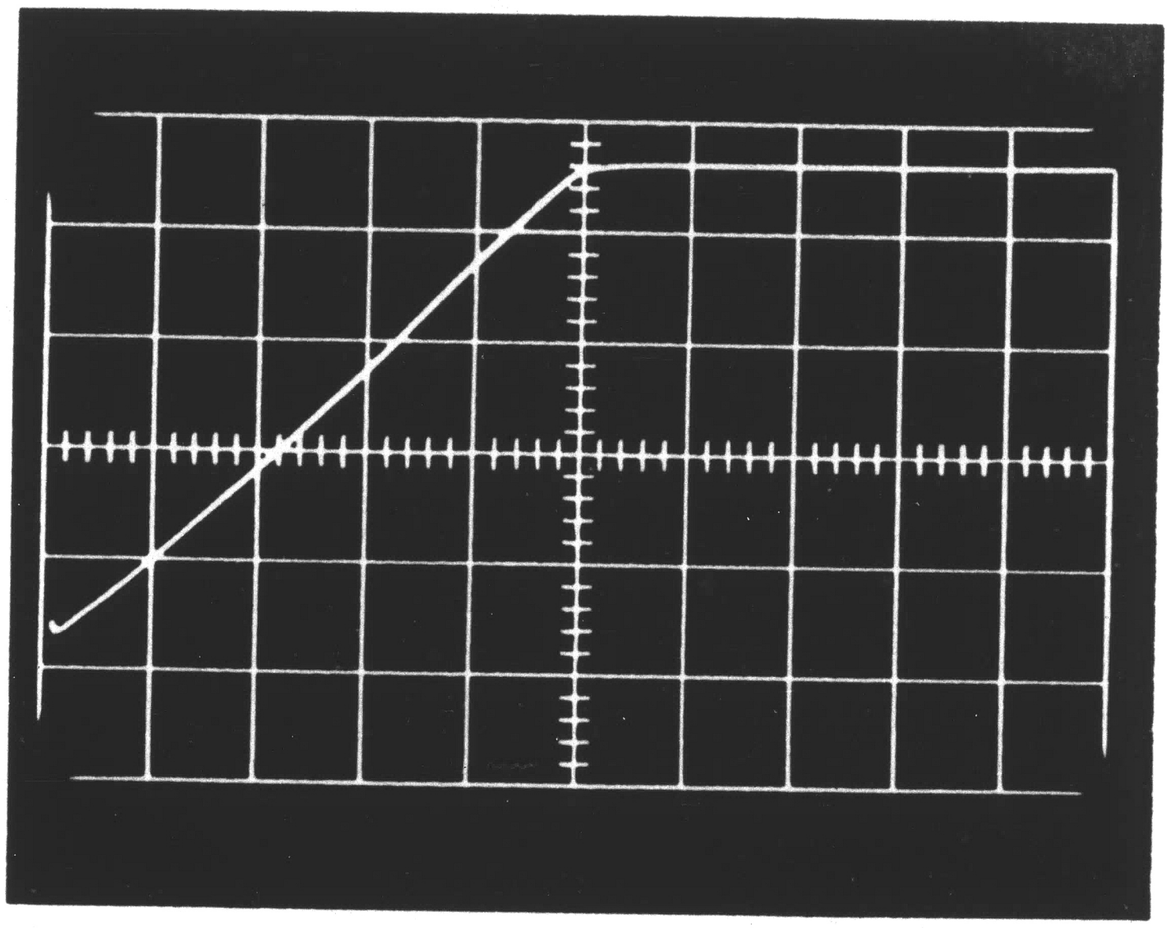

Fig. 5-11. Response of phase stabilization system at the integrator output for a loop gain of 3500 (error = 180°, 1 ms/cm, 20 v/cm).

Figure 5-11 shows, for a gain of 3500, about a 4.0 millisecond increase in response time for an error of 180 degrees.[1] Although long term drift might cause the system to correct for 90 degrees or above, the system would not have to correct for this large an error at one sampling.

5.5 System Correction for Variation of Solenoid Current and Phase Disturbances

In order to measure phase shift under closed-loop conditions, the rf was modulated with a 1000 cycle square wave and a slotted line was used to set up a standing wave as in Figure 5-5. The VSWR meter then detected the 1000 cycles. Any movement of the null position along the slotted line due to solenoid current change or line stretcher (phase) disturbance, can be interpreted as a shift in phase. For the frequency used, 1625 kmc, 1 millimeter is approximately 2 degrees.

Figure 5-12 shows the relative phase shift through the TWT under closed-loop conditions for various values of solenoid current and Figure 5-13 demonstrates the systems ability to correct for disturbances of the line stretcher.

The system was found to correct to about $\pm$ 1 degree accuracy.

1. The method for introducing errors of greater than $|90^{o}|$ is shown in Appendix 5-2.

PHASE SHIFT THROUGH TWT (2) AS A FUNCTION OF SOLENOID CURRENT UNDER CLOSED-LOOP CONDITIONS

f = 1625 KMC

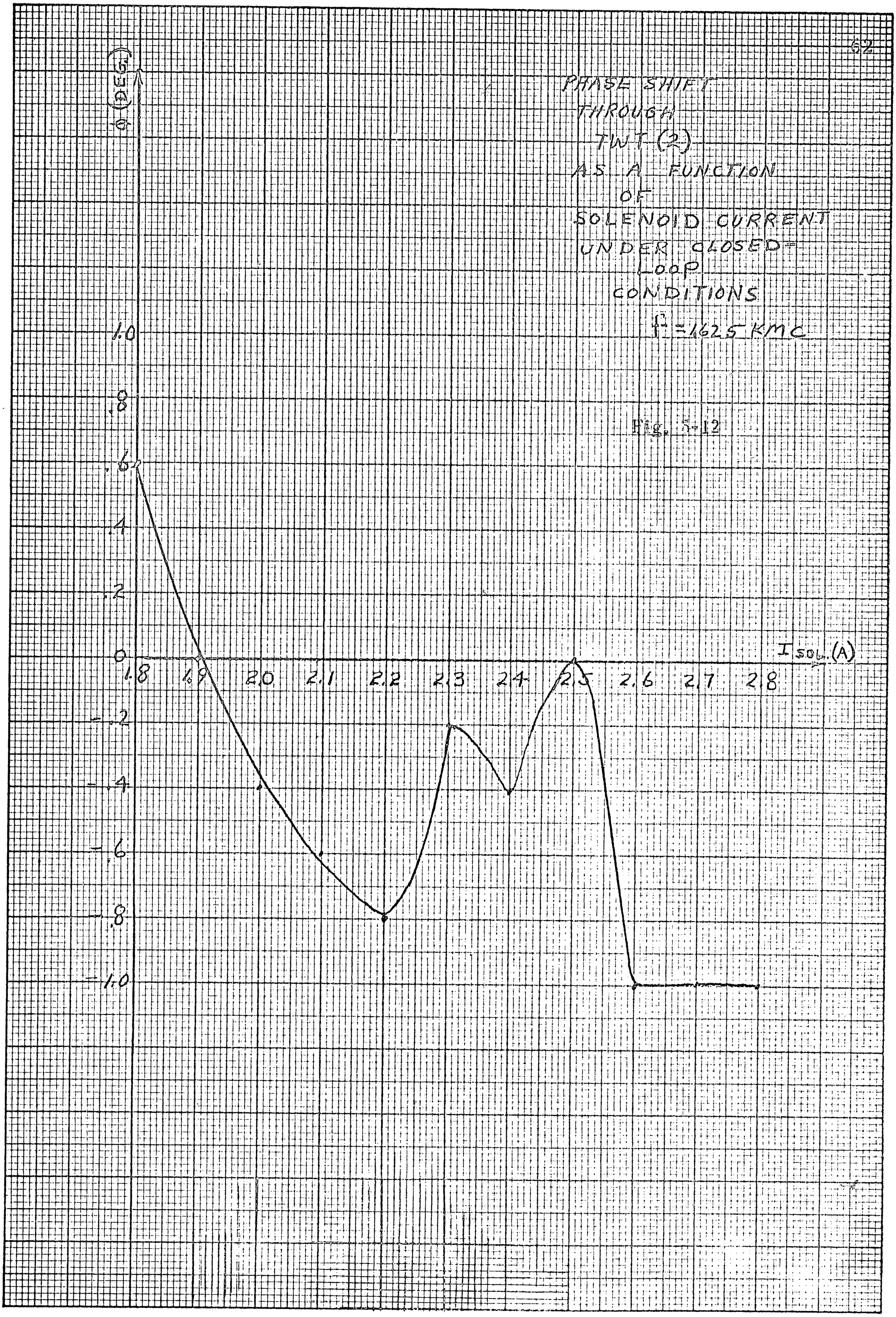

Fig. 5-12

PHASE SHIFT THROUGH TWT(2) FOR VARIATIONS IN LINE STRETCHER LENGTH f=1.625 KMC (CLOSED LOOP)

Fig. 5-13

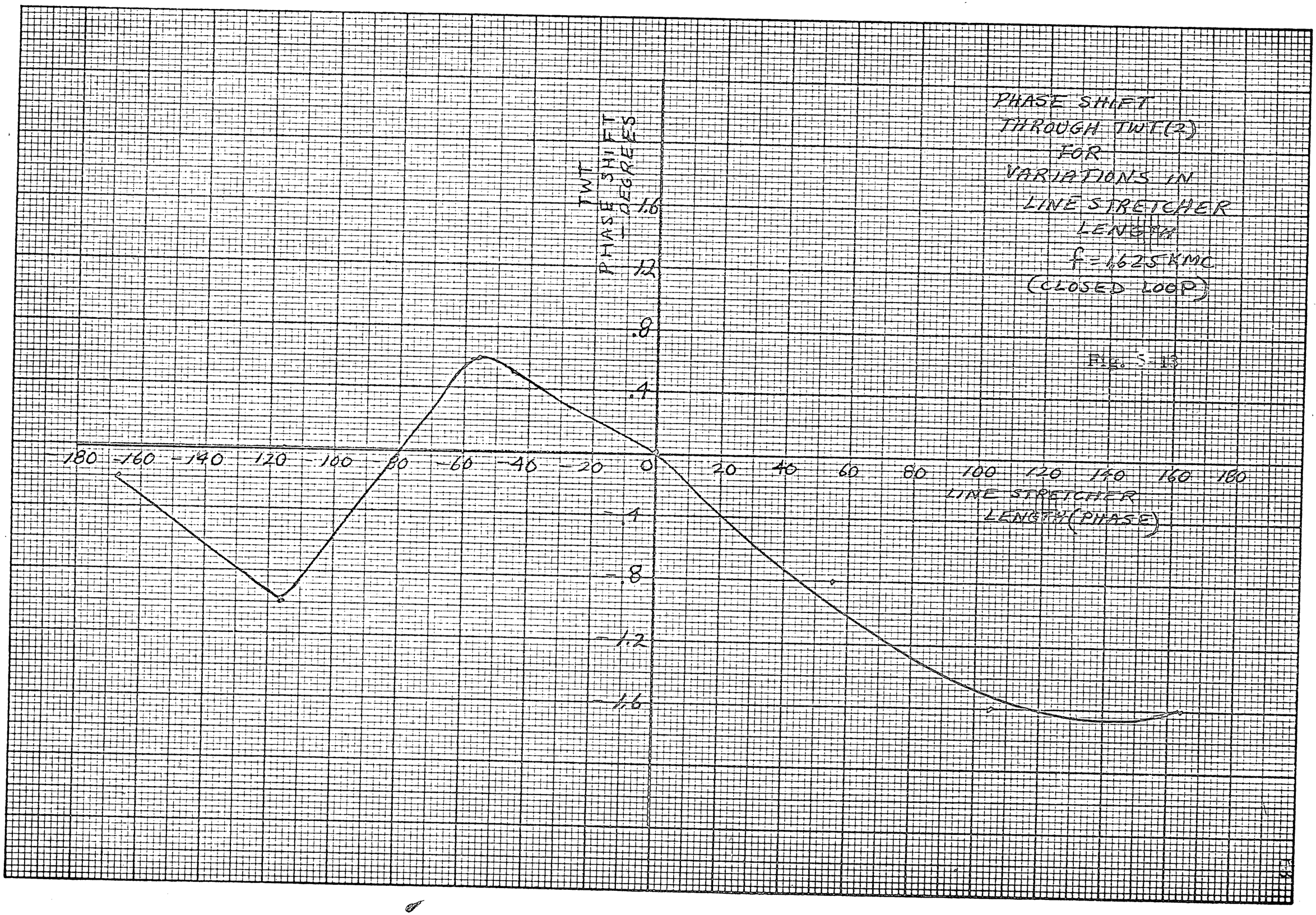

5.6 System Noise

The magnitude of phase noise caused by the feedback system was found to be in the order of $\pm$ 1 degree.

5.7 Phase Disturbances

By monitoring the integrator output voltage, the total phase disturbance for which the system had to correct over a 20 hour period was found to be about 25 degrees and linearly increased from t = 0.

5.8 Integrator Output Decay

The integrator output decay was found to be negligible over a 30 minute sampling time when the forward loop was broken by physically removing the integrator input. For this test a 0.47 uf Vitamin Q Capacitor was used as the integrator feedback capacitor to reduce leakage and the integrator input resistor was effectively infinite because of the means by which sampling took place.

If sampling takes place by grounding the integrator input resistor after the error goes to zero, then the constraints of Section 4.11 would have to be considered. Since, for this case, the theoretical values of decay are in the microvolt range, the experimental results were masked by integrator unbalances. Thus, a comparison of the experimental and theoretical rates of decay was not possible.

However, it was found that for values of integrator input resistance above 100 K ohms, the rate of decay was 0.003 v/sec.[1] This rate was not appreciably sensitive to integrator-balance potentiometer adjustments as was the case for values of resistance below 100 K ohms.

5.9 Conclusions and Recommendations

The designed system successfully stabilized the phase of a traveling-wave tube used as a phase shifter and thus, employment of the closed-loop correction system in a radar is entirely feasible. For 25 degree errors introduced into the system, the response time was found to agree with theoretical expectations. However, because of flatness of the phase detector characteristic around ± 90 degrees, the response time for 180 degree errors was found to be more than 2 times the expected value. The response time for large errors can be improved by improved construction of the coaxial hybrid to give uniformity to all ports. The accuracy of the system's ability to correct for phase drift to within ± 1 degree, as found in Section 5.5, can be improved by utilizing commercial packages available for the operational amplifiers to reduce the noise level. Also, the fact that the null point was defined over a millimeter introduced errors in the readings. Integrator saturation was noticed at the initial turn-on of the feedback system and was improved by reversing the integrator and the adder in the loop. This saturation was caused by unbalances in the adder being integrated during the amplifier stabilization period.

1. Initial rate of decay from 90 V.

For applications where the forward loop will not be broken physically, but perhaps grounded for sampling, it is recommended that the integrator's RC time constant be greater than 50 X 10^{-3} in order to slow the rate of decay of the integrator output voltage during the "radar-on" cycle. This step would necessitate increased gain elsewhere in the loop so that response time would not be degraded.

No effort was made to determine a sampling rate since this characteristic would be governed by the particular radar in which the correction system would be installed.

APPENDICES

APPENDIX 2-1

Derivation of the Phase Sensitivity of the First Anode of a Traveling-Wave Tube[1]

In any electron tube device the three-halves power law for current and voltage is

$$I = KV_1^{3/2} . \tag{1}$$

Therefore

$$\Delta I = \frac{3}{2} KV_1^{1/2} . \tag{2}$$

Dividing the left side by I and the right by $KV_1^{3/2}$,

$$\frac{\Delta I}{I} = \frac{3}{2} \frac{\Delta V_1}{V_1} . \tag{3}$$

According to Pierce,

$$C = K'I^{1/3} . \tag{4}$$

Thus

$$\frac{\Delta C}{C} = \frac{1}{3} \frac{\Delta I}{I} , \tag{5}$$

and

$$\frac{\Delta C}{C} = \frac{1}{2} \frac{\Delta V_1}{V_1} . \tag{6}$$

1. Beam, W. R., and Blattner, D. J., "Phase Angle Distortion in Traveling-Wave Tubes", RCA Review; March, 1956.

Also

$$\beta = \beta_e(1 - Cy) \tag{7}$$

and

$$\Delta\beta = \beta_e(-C\Delta y - y\Delta C) \tag{8}$$

where β_e is constant because of constant helix voltage in this case.

Recalling that

$$\beta_1 = \beta_e(1 + Cb) \tag{9}$$

and taking differentials,

$$0 = \beta_e(C\Delta b + b\Delta C) . \tag{10}$$

From Chapter 2,

$$y = -(.42 + .07\,QC)b - (.5 + .5\,QC); \tag{11}$$

yielding

$$\Delta y = -(.42 + .07\,QC)\Delta b . \tag{12}$$

Combining (6), (8), (10), and (12),

$$\Delta\beta = -\frac{\beta_e \Delta V_1}{2\,V_1} C(y + \left[.42 + .07\,QC\right] b) . \tag{13}$$

From (11)

$$\Delta\beta = +\frac{\beta_e \Delta V_1}{2\,V_1} C\,(.5 + .5\,QC) . \tag{14}$$

Finally, after following the procedure of the derivation of Chapter 2,

$$\Delta\phi = 90\frac{\Delta V_1}{V_1} C\,(1 + QC)\,N \text{ degrees.} \tag{15}$$

APPENDIX 4-1

Derivation of Phase Characteristics for Method 3

From Figure 4-9

$$E_2(s) = E_1(s)G(s) \quad , \tag{1}$$

where G(s) is the closed loop transfer function.

Letting $e^{-\tau s}$ equal a Padé approximation,

$$e^{-\tau s} = \frac{1 - \frac{1}{3}\tau s}{1 + \frac{2}{3}\tau s + \frac{1}{6}\tau^2 s^2} \quad , \tag{2}$$

$$G(s) = \frac{-K e^{-\tau s}}{1 + e^{-\tau s}}$$

$$= -K\left[\frac{1 - \frac{1}{3}\tau s}{1 + \frac{2}{3}\tau s + \frac{1}{6}\tau^2 s^2 + 1 - \frac{1}{3}\tau s}\right]$$

$$= \frac{2K}{\tau}\left[\frac{s - \frac{3}{\tau}}{s^2 + \frac{2}{\tau}s + \frac{12}{\tau^2}}\right] \quad . \tag{3}$$

Let

$$E_1 = \frac{\omega}{s^2 + \omega^2} \quad . \tag{4}$$

Then

$$E_2(s) = \frac{\omega}{s^2 + \omega^2} \left[\frac{s - \frac{3}{\tau}}{s^2 + \frac{2}{\tau} s + \frac{12}{\tau^2}} \right] \frac{2K}{\tau}$$

$$= \left[\frac{\alpha + j\beta}{s + j\omega} + \frac{\alpha - j\beta}{s - j\omega} + \frac{\gamma - j\Delta}{s + \frac{1}{\tau} + j\frac{1}{\tau}\sqrt{11}} + \frac{\gamma + j\Delta}{s + \frac{1}{\tau} - j\frac{1}{\tau}\sqrt{11}} \right] Q \qquad (5)$$

where

$$\alpha = \frac{\frac{9}{\tau^2} - \frac{\omega^2}{2}}{\frac{144}{\tau^4} - \frac{20\,\omega^2}{\tau^2} + \omega^4}, \qquad (6)$$

$$\beta = \frac{\frac{5\,\omega}{2\,\tau} - \frac{18}{\omega\,\tau^3}}{\frac{144}{\tau^4} - \frac{20\,\omega^2}{\tau^2} + \omega^4}, \qquad (7)$$

$$\gamma = \frac{1}{2}\tau^2 \left[\frac{2\sqrt{11}\,(2\,\omega^2\tau^2 - 31)}{11\,\omega^4\tau^4 - 220\,\omega^2\tau^2 + 1584} \right], \qquad (8)$$

$$\Delta = \frac{1}{2}\tau^2 \left[\frac{11\,\omega^2\tau^2 + 198}{11\,\omega^4\tau^4 - 220\,\omega^2\tau^2 + 1584} \right], \qquad (9)$$

and

$$Q = \frac{2K\,\omega}{\tau}. \qquad (10)$$

Taking the inverse Laplace transformation,

$$e_2(t) = \frac{2K\sqrt{\omega^6\tau^6 - 11\,\omega^4\tau^4 - 36\,\omega^2\tau^2 + 1296}}{\tau^4\omega^4 - 20\,\tau^2\omega^2 + 144}\cos(\omega t - \emptyset)$$

$$+ \frac{4K}{\tau} e^{-\frac{t}{\tau}} \sqrt{\gamma^2 + \Delta^2}\,\sin(\omega t + \psi) \qquad (11)$$

where

$$\emptyset = \arctan\frac{\beta}{\alpha}\,, \qquad (12)$$

and

$$\psi = \arctan\frac{\gamma}{\Delta}\,. \qquad (13)$$

The envelope of equation (11) is the desired phase characteristic of method 3.

APPENDIX 5-1

Method for the Determination of Loop Gain

The loop gain of the system was varied by changing the feedback resistor of the operational adder.

For R_1 = 22 K ohms

Gain of integrator $= \frac{1}{RC}$

$= \frac{1}{150 \text{ X } \frac{1}{2} \text{ X } 10^{-6}}$

$= 134 \text{ X } 10^2$.

Gain of helix and phase detector (Measured over linear portion of phase detector characteristics) $= \frac{\text{adder voltage}}{\text{helix voltage}}$

$\approx \pm 0.77$.

Transfer from integrator to helix $= \frac{1}{K_{ps}}$

$= .34$.

Thus, the total loop gain for R_1 = 22 K ohms is

$$K = (134 \text{ X } 10^2)(.77)(.34)$$

$$= 3500.$$

For other values of R_1, R_1', the loop gain is

$$K = \frac{R_1'}{R_1} 3500.$$

APPENDIX 5-2

Introduction of Errors of Greater Than $|90^{o}|$

The method for introducing square wave errors at the input of the integrator breaks down over $|90^{o}|$ due to the non-linearity of the phase detector. Thus for errors above $|90^{o}|$, the square wave voltage would have to be lowered to simulate these larger errors. Of course, this is just the case for errors less than $|90^{o}|$.

To simulate 180 degree errors, the r f was removed and slight unbalances caused the integrator output to drift. When the drift was such to cause 180 degree phase shift through the TWT, the r f was turned on and the system correction was recorded by monitoring the return of the integrator voltage to zero.

BIBLIOGRAPHY

1. Albanese, V. J., Kagan, H., "The 'Cross-Over' Directional Coupler", The Microwave Journal, Vol. 4, No. 9; September, 1961.

2. Beam, W. R. and Blattner, O.J., "Phase Angle Distortion in Traveling-Wave Tubes"; RCA Review; March, 1956.

3. Bellis, D. R., Huggins, R. A., "Phase Modulation of Traveling-Wave Tubes", Huggins Laboratories Engineering Notes No. 7, Sunnyvale, California; March, 1957.

4. Bray, W. J., "The Traveling-Wave Valve as a Microwave Phase-Modulator and Frequency-Shifter", Proc. Inst. Elect. Engrs.Part III, Vol. 99; January, 1952.

5. Gille, J. C., Pelegrin, M. J., Decaulne, P., "Feedback Control Systems", McGraw-Hill, New York, N.Y.; 1959.

6. Heitzman, E. J., "Operation of Traveling-Wave Tubes", Electrical Design News; September, 1960.

7. King, D.D., Barrack, C.M., Johnson, C. M., "Precise Control of Ferrite Phase Shifters", IRE Trans. on Microwave Theory and Techniques"; April, 1959.

8. Loth, P. A., "Recent Advances in Waveguide Hybrid Junctions", IRE Transactions on Microwave Theory and Techniques; October, 1956.

9. McIsaac, P. R., Eastman, L. F., Engler, P. E., "Phase Stability Measuring Set", School of Electrical Engineering, Cornell University Research Report EE460, Ithaca, N.Y.; January 20, 1960.

10. Olin, I. D., "The Traveling-Wave Tube as a Phase Shifter", Naval Research Laboratory Report 4026, Washington, D. C.; July 29, 1952.

11. Pierce, J. R., "Traveling-Wave Tubes", D. Van Nostrand, New York, N.Y.; 1950.

12. RCA Electron Tube Division, "RCA Magnetrons and Traveling-Wave Tubes", Harrison, N.J.; 1960.

13. Research Laboratory of Electronics, MIT, "Phase Stabilization Techniques for Electronically Scanned Arrays", Quarterly Technical Note No. 1, AD-148961, Cambridge, Mass.; September 15, 1958.

14. Research Laboratory of Electronics, MIT, "Phase Stabilization Techniques for Electronically Scanned Arrays", Quarterly Technical Note No. 2, AD-209072, Cambridge, Mass.; December 15, 1958.

15. Research Laboratory of Electronics, MIT, "Phase Stabilization Techniques for Electronically Scanned Arrays", Quarterly Technical Note No. 3, AD-213587, Cambridge, Mass.; March 15, 1959.

Norman Saul Nise, son of Mr. and Mrs. Frank Nise, was born in Philadelphia on September 16, 1937. He received his B. S. in Electrical Engineering Degree in 1960 from Drexel Institute of Technology where he became a member of Eta Kappa Nu and President of Tau Beta Pi. He was employed by Remington Rand Univac as a cooperative student for a total of 2 years while an undergraduate.

He attended Lehigh University under a C. Kemble Baldwin Fellowship where he received his M. S. in Electrical Engineering in 1962.

Presently, Mr. Nise is working at Hughes Aircraft Company in the Ground Systems Group as a Member of the Technical Staff of the Radar Laboratory.